KU-Synapse 2026

“Psycho-Brain Networking”

뇌공학과 – 심리학부 공동 워크숍

연구 역량 공유와 공동 연구 기반 마련을 위한 만남

뇌공학과와 심리학부가 함께 모여 서로의 연구를 이해하고,
새로운 아이디어와 협력의 가능성을 발견하는 교류의 장을 마련합니다.

- 연구 교류
- 협력 기회
- 융합 시너지
- 미래 연구

June 30
Tuesday 2026
13:00 – 16:30

고려대학교

하나스퀘어
아뜨리움

ORGANIZER

ABCE RC
ADVANCED BRAIN AND COGNITIVE ENGINEERING RESEARCH CONSORTIUM

고려대학교 4단계 BK21 심리학 교육연구단
Korea University
BK21 FOUR R&E Center for Psychology

SPONSOR

고려대학교
KOREA UNIVERSITY

Abstract & Posters

Number	Title	Submitting author
#01	Social Comparison Tendencies Predict Heart Rate Responses to Social Evaluation	Jinhee Kim
#02	Midfrontal Neural Excitability: Distinct EEG Correlates of Executive Function and Autism Features	Suhyoung Jeong
#03	Interoceptive sensitivity shapes the temporal dynamics of emotional interference and enhances negative memory consolidation	Hyeyoon Jung
#04	BrainDynDiff: Spatiotemporal fMRI-Guided Latent Diffusion for Multi-Tracer PET Synthesis	Hwapyeong Baek
#05	Establishment of Focused Ultrasound (FUS) Parameters for Neuromodulation	Seoyeon Hong
#06	Selective reduction of anxiety-like behavior and modulation of c-Fos activation via ketone-supplemented diet in rats	Ju Young Choi
#07	Why Do We Sabotage Ourselves?: Social Evaluation, Interoception and Cultural Adaptation in Self-Handicapping	Kyunghwan Lee
#08	Altered Cortical Hierarchical Organization In ADHD	Seoah Lee
#09	Multimodal fusion approaches for investigating discrete and continuous dimensions of Alzheimer's disease	Taeyeon Kim
#10	Activation of Prefrontal SST Neurons Rescues the Immediate Extinction Deficit	Kyeong Im Jo
#11	Object and Background contributions to neural representations in natural images	Suhyun Kim
#12	Associations of spatial gradients between magnetoencephalography and magnetic resonance imaging	Ju Hyung Lee
#13	The Role of Recurrent Connections in Holistic Face Processing	Jiwon Kim
#14	Diagnosing Neural-Signal Dependence in Subject-General fMRI-to-Language Decoding	Sunghwan Lee
#15	Whole-Brain Decoder-Based Real-Time fMRI Neurofeedback: Strengthening the Interoceptive Salience Network	Jihun Kim
#16	State-dependent associations between perceptual dimensions of electric vehicle driving sounds and attentional response speed	Chaelynn Kim
#17	Differences in HRV Across Task Types During Home-Based Introceptive Training	Joungwoo Choi
#18	The Priming Effect of the Korean Adnominal Transformation Suffix "-ㄴ" in Phrase Parsing: A Lexical Decision Task Study	Taeryung Kim
#19	Investigation of the Mechanisms of Cross-Modal Congruency Sequence Effect: A Diffusion Model Analysis	Jin Ho Kim

Abstract & Posters

Number	Title	Submitting author
#20	Decoding Visual Event Captions from 7T Naturalistic Movie-watching Brain via 4D fMRI Encoding and Persistent Cross-Attention	Ji-Yun Park
#21	Preliminary Physiological and Resting-State Connectivity Trends During Interoceptive Neurofeedback Training	Jae-eon Kang
#22	Heartbeat-Evoked Potentials Across Interoceptive, Resting and Diverse Cognitive States: An EEG-fMRI Study	Changha Lee
#23	Behavioral Assessment Identifies Line-Dependent Susceptibility to Novelty-Induced Memory Enhancement	Eunjin Paek
#24	VTA-to-CeA Dopamine Release Is Linked to Appropriate Action Selection During Active Avoidance	Eunsol Cho
#25	Behavioral and Electrophysiological Evidence for Early Suppression of Singleton Distractors	Si Eun Choi
#26	Neural and Behavioral Effects of In-Phase Frontoparietal Theta tACS on Working Memory in Middle-Aged Adults	Hyeong Ha Kim
#27	Functional brain asymmetry reveals heterogeneous subtypes in autism spectrum disorder	Chaeyeon Kim
#28	Post-Conflict Adjustments Following Infrequent Responses: A Drift Diffusion Modeling Approach	Jaewon Han
#29	Cognitive Learner Profiles in Repeated L2 Grammar Practice: A Machine-Learning Approach Using SVT and MAZE Tasks	Sungyeop Ha
#30	REV-ERBα Activation Reduces Dopamine Release and Addictive Behavior	Jihyun Lee
#31	Dissociable Neural Representations in mPFC Subregions during Self- vs. Other-Referenced Social Comparison	Sa Im Kim
#32	Modeling Reward Value- and Outcome Uncertainty-Driven Attentional Capture Using DDM	Jaein Lee
#33	Age-Related Differences in Working and Episodic Memory: Effects of Emotional Valence on Mean Performance and Within-Group Performance Heterogeneity	Jungmin Oh
#34	Repetitive transcranial magnetic stimulation reorganizes functional connectome manifolds	Sunghun Kim
#35	The Impact of Time Pressure on Hierarchy-Based Conformity: The Moderating Role of Interoceptive Accuracy	Sanghun Kim
#36	Congruency Sequence Effects Optimize Real-Time Motor Correction in spatial Stroop Conflict	Yeong Sun Heo
#37	Validating the Mirroring Hypothesis: The Impact of Perceived AI Identity on Free-Form Conversational Engagement and Assimilation	Inseun Kim

Abstract & Posters

Number	Title	Submitting author
#38	Ampakines CX516 and CX717 Selectively Enhance Cued Fear Learning, as Revealed by Behavioral Characterization	Seongmin Kwon
#39	Reliability-Aware Rejection over Multimodal Fusion for Camera and IMU-Based Respiratory Rate Estimation	Minwoo Lee
#40	Mobile-based facial emotion perception training (moFEPT) influences attentional processing	Sue Yeon Ko
#41	Cortical responses to heartbeats predict alignment with group consensus in moral and affective preference	Juyoung Kim
#42	Neural Mechanisms Linking Interoception and Subjective Preference: Evidence from EEG and fMRI	Hackjin Kim
#43	Superlet-MAE: Self-Supervised Masked Autoencoding for Sleep Staging Using Single-Channel EEG	Jeong-Yun Cha
#44	Population analyses reveal heterogenous encoding in the medial prefrontal cortex during naturalistic foraging	June-Seek Choi
#45		
#46		
#47		
#48		
#49		
#50		

[#01]

Social Comparison Tendencies Predict Heart Rate Responses to Social Evaluation

Jinhee Kim[1], Gahyun Lim[1], Jihwan Chae[1], Hackjin Kim[1]*

[1]School of Psychology, Korea University, Seoul, South Korea

Social comparison is a pervasive aspect of everyday life, particularly in social media contexts. While it is known to affect mental health and produce autonomic physiological responses, its underlying peripheral physiological signatures and their associations with individual differences in social comparison behavior remain poorly underexplored. This study investigated cardiac responses to social comparison outcomes and the associations of these responses with individual differences in social comparison behavior, with the role of interoceptive ability in social comparison sensitivity additionally explored. A total of 132 participants engaged in a social evaluation acceptance task using a smartphone application while their cardiac activity continuously monitored via a smartwatch. Participants were informed that raters from a multi-user metaverse would rate their likability. In each trial, participants viewed likability scores from a rater for themselves and a partner: absolute and relative social evaluative outcomes were manipulated independently. Social comparison tendency was quantified by the degree to which relative ratings influenced participants' decisions to accept an evaluation outcome. Additionally, interoceptive accuracy and metacognition were assessed using a heartbeat counting task. Behavioral results showed that participants' decisions to accept evaluation outcomes were influenced by both absolute and relative rating, with social comparison effects being more pronounced in negative contexts. Cardiac time-series analysis revealed that relative ratings significantly modulated phasic cardiac deceleration, with greater heart rate slowing observed in response to relatively inferior social evaluation outcomes. Individual differences in cardiac responses to relatively favorable outcomes in negative contexts were associated with behavioral sensitivity to social comparison. Intersubject representational similarity analysis confirmed that individuals with similar behavioral profiles exhibited analogous cardiac response patterns across conditions. Finally, exploratory analyses suggested that a higher social comparison tendency was associated with lower interoceptive metacognition. These findings provide novel psychophysiological evidence that social comparison processes elicit distinct cardiac responses, which in turn reflect individual sensitivity to social comparison.

[#02]

Midfrontal Neural Excitability: Distinct EEG Correlates of Executive Function and Autism Features

Suhyoung Jeong[1], Boin Choi[2], Yael Braverman[3], Natasha Bertelsen[4], Jeongjin Kim[5], Seok-Jun Hong[6], Michael Lombardo[4], Susan Faja[7], So Hyun Kim[1]

[1]School of Psychology, Korea University, Seoul, South Korea
[2]Department of Special Education, Ewha Womans University, Seoul, South Korea
[3]Pomelo Care, New York, NY, USA
[4]Laboratory for Autism and Neurodevelopmental Disorders, Center for Neuroscience and Cognitive Systems, Istituto Italiano di Tecnologia, Roverto, Italy
[5]Center for Neuroscience, Brain Science Institute, Korea Institue of Science and Technology, Seoul, South Korea
[6]Department of Biomedical Engineering, Sungkyunkwan University, Seoul, South Korea
[7]Laboratories of Cognitive Neuroscience, Division of Developmental Medicine, Harvard Medical School, Boston Children's Hospital, Brookline, MA, USA

Electroencephalography (EEG) studies have begun to unravel neural mechanisms underlying core features of autism and cognitive processes such as executive function (EF). The SpecParam (formerly known as Fitting Oscillations and One-Over-F; FOOOF; Donoghue et al., 2020) algorithm allows separation of periodic (oscillatory) and aperiodic (1/f-like) components of EEG power spectra, enabling refined analysis of cortical excitatory/inhibitory (E/I) balance and alpha oscillations linked to cognitive processing (Leno et al., 2022; Samaha et al., 2024). Based on resting-state EEG in autistic and neurotypical kindergarteners, we aimed to: (1) identify group differences in aperiodic and periodic EEG components, and (2) to assess how these components predict individual differences in core autism symptoms and EF. Participants were 212 cognitively-able (NVIQ≥85), fluent-speech kindergarteners (100 autistic, 112 neurotypical, Mean Age=69.6 months). We collected 5-minute resting-state EEG (mid-frontal cluster), performance on tablet-based EF tasks ("EF Touch" Willoughby et al., 2010) measuring inhibition (Spatial Conflict Arrows; SCA) and attention shifting (Something's the Same; STS), and autism symptom severity via the ADOS-2 Calibrated Severity Score for the Social Affect (SA) and Restricted and Repetitive Behaviors (RRB) domains separately (Hus et al., 2014). Aperiodic and periodic parameters were extracted using the SpecParam algorithm. A covariate-controlled linear regression model tested for diagnostic group differences in EEG. Stepwise AIC linear regression models identified the most salient EEG predictors of autism symptoms (with ASD) and EF (for both ASD and NT). All mid-frontal aperiodic (slope, offset) and periodic alpha band components (center frequency, power, bandwidth) were considered. All models controlled for age, gender, NVIQ, and site (for symptom prediction models) as well as diagnosis (for EF prediction models). Autistic children showed a significantly flatter aperiodic slope (greater broadband excitation) compared to their neurotypical peers (β=−0.04, p=.02), which predicted higher ADOS-2 CSS-RRB scores within the autistic group (β=−0.38, p=.03). Though offset did not differ by diagnosis, higher offset (greater broadband arousal) was associated with both increased CSS-RRB (β=0.59, p<.01) and better EF task performance (STS: β=0.03, p<.01; SCA: β=0.03, p=.04). Among periodic components, lower alpha power (greater oscillatory excitation) predicted better STS scores (β=–0.02, p=.04), while greater alpha bandwidth (greater oscillatory instability) predicted greater CSS-RRB in autistic children (β=0.43, p=.01). We used the SpecParam algorithm to separate aperiodic and periodic components to investigate their respective contributions to autism symptoms and EF using resting EEG data from young children. A flatter aperiodic slope—suggesting broadband E/I imbalance—emerged as a neurophysiological signature distinguishing young autistic children and was associated with higher RRBs. A higher offset, indicative of increased broadband neural readiness, was also related to greater RRBs and better EF, suggesting that heightened neural activity linked to RRBs may, in some contexts, facilitate cognitive engagement. Alongside aperiodic components, greater oscillatory excitation (lower alpha power) predicted better EF skills, while greater oscillatory instability (alpha bandwidth) was associated with higher RRBs. Given the past findings showing the associations between RRBs and EF (Iversen et al., 2021), these constructs may share overlapping or interacting neural mechanisms.

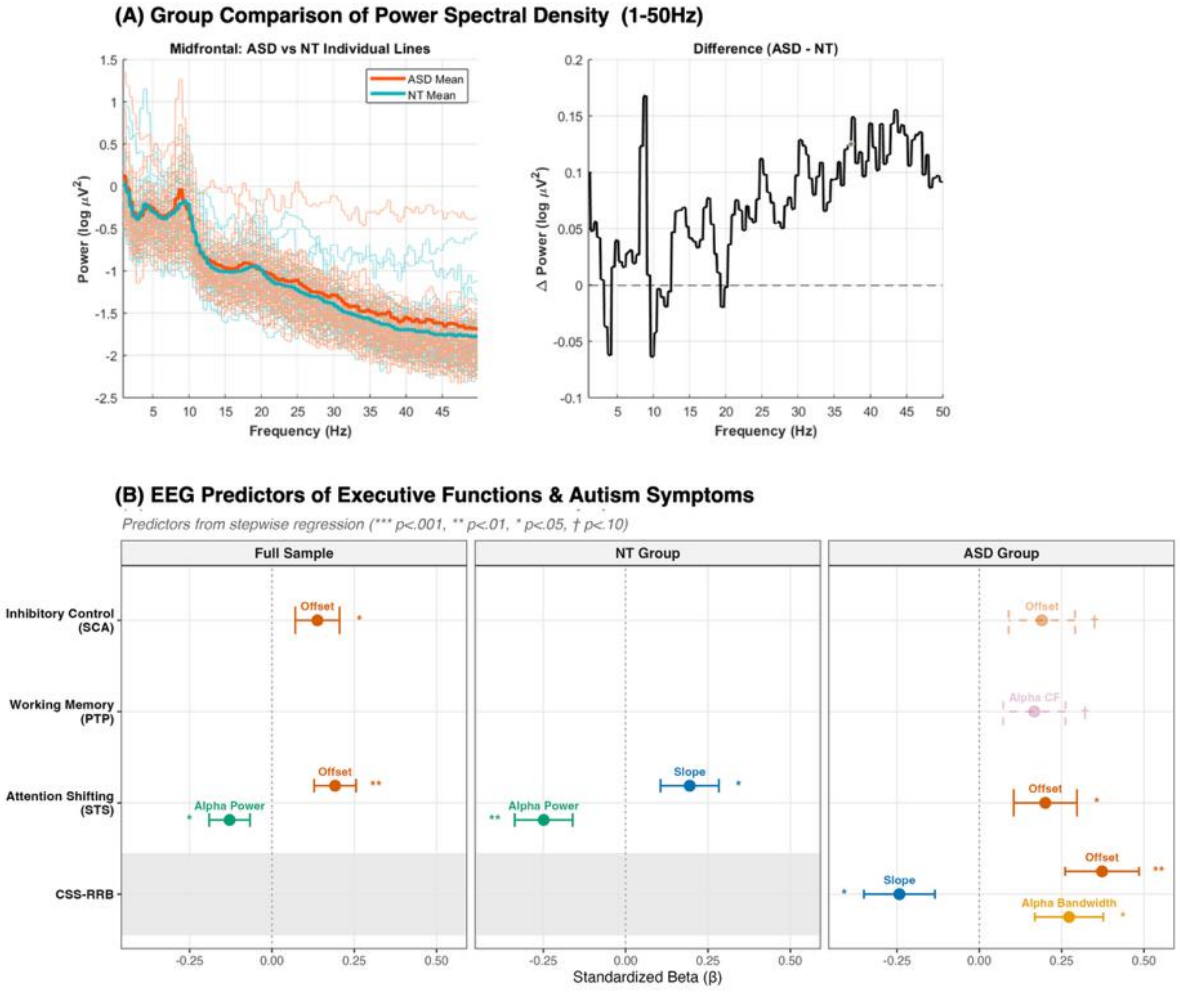
(A) Group Comparison of Power Spectral Density (1-50Hz)
Midfrontal: ASD vs NT Individual Lines
ASD Mean
NT Mean
Power (log μV²)
Frequency (Hz)
Difference (ASD - NT)
Δ Power (log μV²)
Frequency (Hz)
(B) EEG Predictors of Executive Functions & Autism Symptoms
Predictors from stepwise regression (*** p<.001, ** p<.01, * p<.05, † p<.10)
Full Sample
NT Group
ASD Group
Inhibitory Control (SCA)
Working Memory (PTP)
Attention Shifting (STS)
CSS-RRB
Offset
Alpha Power
Slope
Alpha CF
Alpha Bandwidth
Standardized Beta (β)

[#03]

Interoceptive sensitivity shapes the temporal dynamics of emotional interference and enhances negative memory consolidation

Hyeyoon Jung[1], Yuri Kim[1], Hackjin Kim[1]

[1]School of Psychology, Korea University, Seoul, Korea

Interoception, the perception of internal bodily signals, is a fundamental component of emotional experience, with higher interoceptive sensitivity often linked to more intense emotional processing. Although individuals with greater interoceptive sensitivity exhibit stronger emotional interference—evidenced by delayed responses to negative versus neutral stimuli—the temporal dynamics of this phenomenon remain poorly understood. Because emotion is a dynamic process that unfolds over time, this study investigated how temporal trajectories of emotional interference vary with interoceptive sensitivity and how these temporal changes subsequently shape emotional memory. Fifty-one young Korean adults completed a Heartbeat Counting Task to assess interoceptive accuracy as an index of interoceptive sensitivity. They then performed a modified color-word emotional Stroop task, followed by an unexpected word memory test. Results showed that negative stimuli elicited a slow and transient interference effect, whereas positive stimuli produced a fast and sustained facilitation effect. Notably, individuals with higher interoceptive sensitivity exhibited stronger interference for negative stimuli during both early (r = .43, p = .007) and later phases (r = .33, p = .045). Furthermore, greater late-phase interference predicted enhanced memory for negative stimuli (r = .40, p = .018), and interoceptive sensitivity influenced memory indirectly by amplifying this late interference (indirect effect = .13, p = .028). These findings suggest that interoceptive sensitivity shapes not only the initial impact of emotional stimuli but also their temporal unfolding and subsequent consolidation into memory. By examining the precise time course of emotional interference, this study advances our understanding of the dynamic role of interoception in emotional processing and highlights brain-body interactions underlying these temporal dynamics.

[#04]

BrainDynDiff: Spatiotemporal fMRI-Guided Latent Diffusion for Multi-Tracer PET Synthesis

Hwapyeong Baek[1], Jae-Ho Han[1*]

[1]Department of Brain and Cognitive Engineering, Korea University, Seoul, Korea

Positron emission tomography (PET) is the gold standard for characterizing amyloid-β pathology in Alzheimer's disease (AD). However, high costs, infrastructure requirements, and radiation exposure limit its routine clinical use and the frequency of longitudinal monitoring. While conventional deep learning frameworks for MRI-to-PET synthesis offer a non-invasive alternative, they rely primarily on structural MRI (sMRI). Consequently, these structure-only models fail to capture the early functional network alterations that are intrinsically coupled with prodromal AD pathology before macroscopic atrophy becomes evident. To address this critical gap, we propose BrainDynDiff, a spatiotemporal fMRI-guided latent diffusion framework for amyloid PET synthesis. Operating within a Latent Brownian Bridge Diffusion Model (BBDM), BrainDynDiff unifies the morphological precision of sMRI with the dynamic neural trajectories of 4D resting-state fMRI. We engineered a Dynamic BOLD Encoder utilizing a per-position Bidirectional Mamba (BiMamba) architecture. This allows for linear-time spatiotemporal modeling that preserves whole-brain functional topology without truncating essential long-range temporal dependencies. Furthermore, we introduced a hierarchical conditioning mechanism. By integrating a Feature-wise Linear Modulation (FiLM) bottleneck for global temporal context and Spatially Adaptive Denormalization (SPADE) layers for localized voxel-level guidance, our model accurately maps the distinct topography of amyloid deposition (Figure 1). Evaluated on 463 subjects from the ADNI cohort, BrainDynDiff significantly outperforms established structure-only generative baselines (Table 1). By leveraging uncompressed functional dynamics, our framework achieves substantial improvements in both voxel-level image fidelity and regional clinical biomarker alignments. Notably, functional conditioning yielded pronounced accuracy gains in amyloid-sensitive regions (e.g., precuneus and posterior cingulate cortex), corroborating the hypothesis that early amyloid accumulation is tightly coupled to highly active functional hubs. Interpretability analysis of the spatial feature maps confirmed that the model actively focuses on the Default Mode Network (DMN), biologically validating its capability to infer pathological vulnerability from latent BOLD dynamics. BrainDynDiff successfully establishes resting-state fMRI BOLD dynamics as a biologically informative prior for guiding amyloid PET synthesis. By providing a highly accurate, radiation-free, and cost-effective computational surrogate for visualizing amyloid-β distribution, this framework offers significant potential for early AD risk stratification and accessible longitudinal screening.

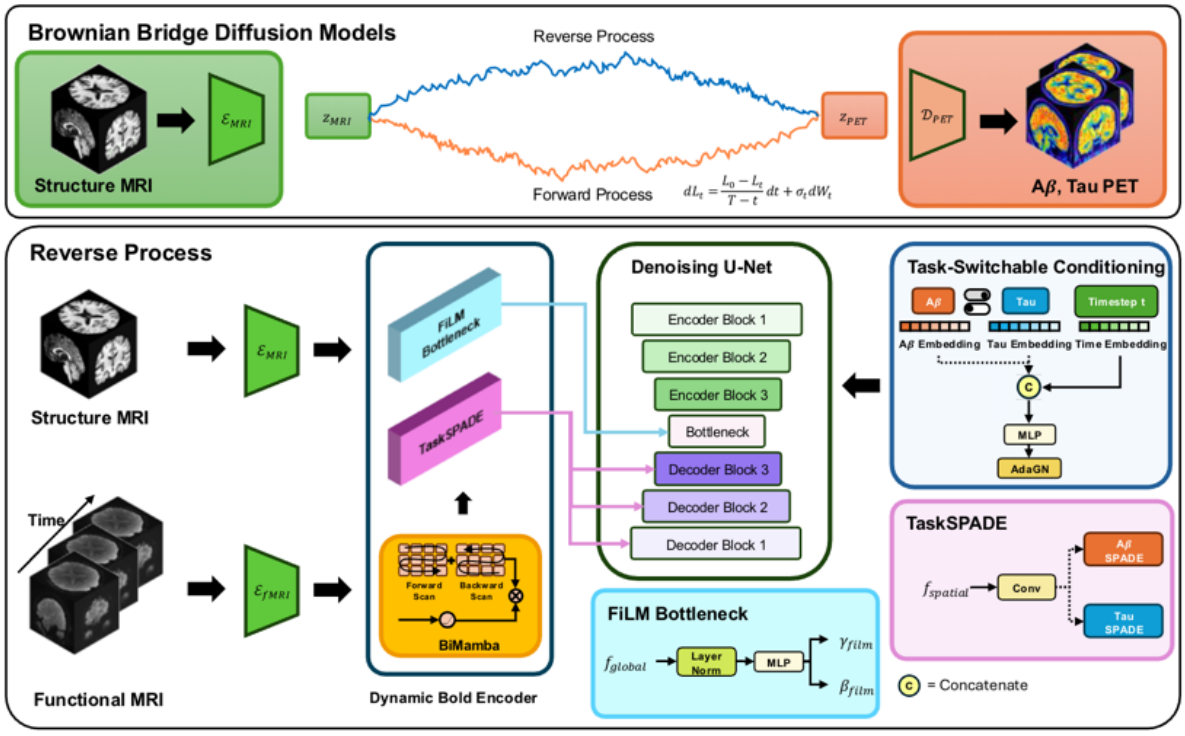

Figure 1. Overall architecture of BrainDynDiff.

Table 1. Quantitative comparison of amyloid PET synthesis performance. The best results are highlighted in bold.

Method	Modality	MAE ↓	rRMSE[%] ↓	PSNR ↑	SSIM ↑	PCC-V ↑	PCC-ROI ↑
Pix2Pix	MRI	72.38	122.33	17.44	0.762	0.825	0.733
CycleGAN	MRI	75.62	117.02	17.06	0.733	0.783	0.697
ResViT	MRI	78.23	127.92	16.90	0.742	0.792	0.723
SwinUNETR	MRI	68.36	110.36	18.44	0.778	0.852	0.768
LDM	MRI	118.10	192.21	12.82	0.672	0.587	0.356
ALDM	MRI	72.78	116.76	17.46	0.737	0.762	0.630
BBDM	MRI	68.76	110.74	18.20	0.782	**0.854**	0.773
BrainDynDiff *(Ours)*	MRI+fMRI	**65.30**	**105.70**	**18.52**	**0.782**	0.852	**0.783**

[#05]

Establishment of Focused Ultrasound (FUS) Parameters for Neuromodulation

Chengxin Zhang[1, 2*], Seoyeon Hong[1,2*], Gyurin Kim[1,2*], Jihyun Shin[1,2], Sangmun Hwang[1,2], Seyoung Choi[2,3], Jinwoo Chang[2,3], Yoonbae Oh[1,2]

[1]Department of Brain & Cognitive Engineering, Korea University, Korea
[2]Neural Engineering for Precision Surgery Laboratory, Korea University, Seoul, Korea
[3]Department of Neurosurgery, Korea University Anam Hospital, Seoul, Korea
*These authors contributed equally to this work.

Compulsive overeating shares key neurobiological mechanisms with substance use disorders, driven by dysregulation of the mesolimbic dopaminergic system. The pathology is characterized by a low dopaminergic state, including reduced striatal D2 receptor availability and imbalance between phasic dopamine transients and tonic baseline levels. Deep Brain Stimulation (DBS) targeting reward circuitry has shown therapeutic potential but is limited by high invasiveness. This study proposes a non-invasive neuromodulation approach using Low-Intensity Focused Ultrasound (LIFU) to restore dopaminergic balance. The study aims to detect significant increases in both basal (tonic) and phasic dopamine levels. The goal is to establish a novel, non-invasive therapeutic protocol using focused ultrasound (FUS) to validate a dopamine deficiency model of food addiction. We have demonstrated a technical framework for the precise and non-invasive targeting of the mesolimbic dopaminergic system using FUS. By mapping precise stereotaxic coordinates for Bregma, MFB, VTA, and M1, we have ensured the anatomical accuracy required for reliable neuromodulation in future in vivo studies. Our parameter optimization process indicates that this non-invasive approach can significantly reduce surgical risks compared to DBS. This study is strategically designed to incorporate M-CSWV and FSCV, enabling simultaneous tracking of basal and phasic dopamine fluctuations. The progress provides a foundation for investigating dopaminergic dysregulation and validating therapeutic strategies for food addiction. Future research will focus on implementing real-time neurochemical monitoring and observing long-term behavioral changes to establish a standardized non-invasive clinical protocol.

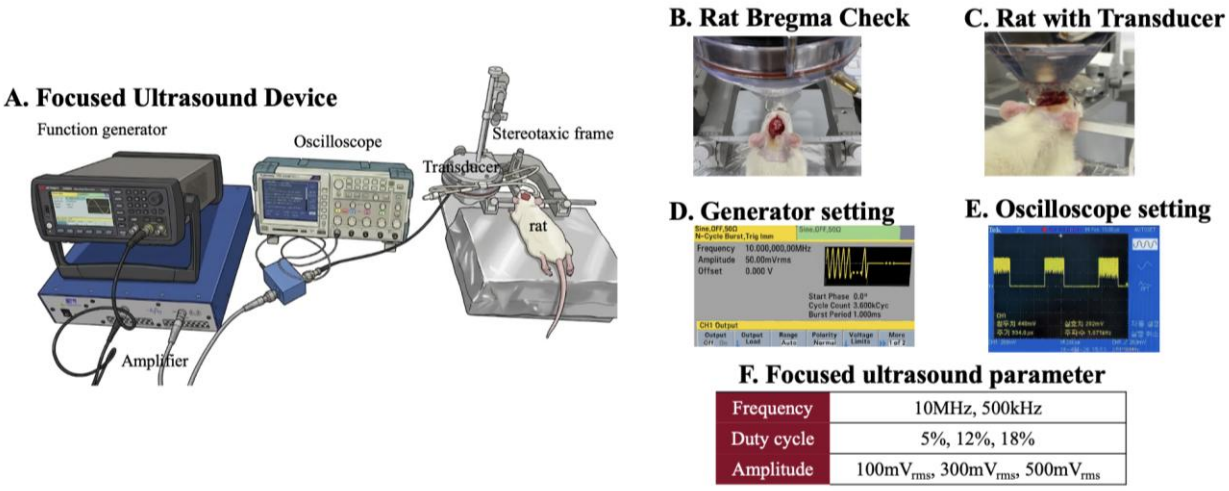

F. Focused ultrasound parameter

Frequency	10MHz, 500kHz
Duty cycle	5%, 12%, 18%
Amplitude	100mV$_{rms}$, 300mV$_{rms}$, 500mV$_{rms}$

Figure 1. FUS setting. (A) The signal flow proceeds from the Function generator through an Amplifier, with the amplified output simultaneously delivered to the Transducer and monitored by the Oscilloscope. (B) Setting up a rat in the stereotaxic frame with bregma exposed. (C) Application of ultrasound gel and positioning of the transducer in close contact with the target area. Calculation of FUS parameters tailored to specific brain regions, intensities, and duty cycles, and subsequent input into the FUS device. (D) Function generator display showing a 10MHz frequency, 500kHz amplitude, and 36% duty cycle. (E) Oscilloscope display verifying the actual signal output with a measured 36% duty cycle. (F) Focused ultrasound parameter values input to the generator

Table 1. Stereotaxic coordinates. Stereotaxic setup for targeting MFB, M1, and VTA based on precise coordinates relative to Bregma.

	Bregma	MFB
ML	38.9	1.4
AP	51.5	-4.8

	Bregma	M1	VTA
ML	38.4	3	0.8
AP	61.5	2	-5

[#06]

Selective reduction of anxiety-like behavior and modulation of c-Fos activation via ketone-supplemented diet in rats

Ju Young Choi[1], Yong Sang Jo[1], June-Seek Choi[1]

[1]Department of Psychology, Korea University, Seoul, Korea

Although various studies have shown that ketogenic interventions reduce anxiety-like behavior, those effects have primarily been demonstrated in pathological models, and the underlying neural mechanisms remain unclear. To evaluate the effects of ketone supplementation, a voluntary ketone-supplemented diet was provided ad libitum to Sprague-Dawley rats. The ketone-supplemented diet successfully induced nutritional ketosis and selectively reduced anxiety-like behavior without affecting other behaviors. A separate cohort was used to assess c-Fos activity after ketone supplementation and exposure to the elevated plus maze test. The ketone group showed increased c-Fos activation in the arcuate nucleus of the hypothalamus and attenuated c-Fos activation in the bed nucleus of the stria terminalis and the central nucleus of the amygdala.

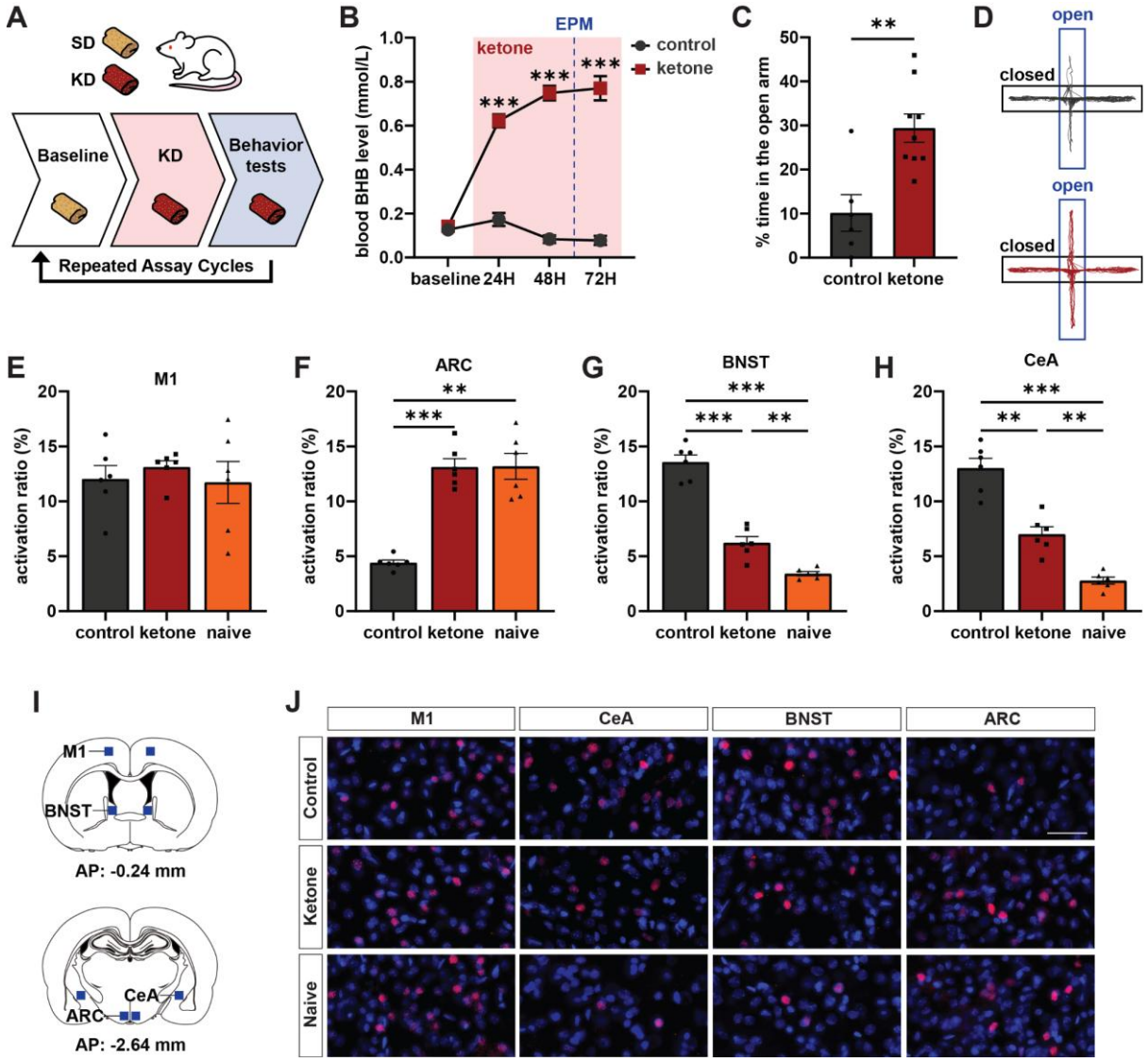

Figure 1. Ketone supplementation induces nutritional ketosis, reduces anxiety-like behaviors, and modulates neural activation. (A) Experimental timeline for Experimental 1 and a schematic of the diet conditions (SD, standard diet; KD, ketone-supplemented diet). (B) Longitudinal monitoring of blood BHB concentrations across the baseline and the 72-hour dietary intervention period. (C) Percentage of the time spent in the open arms of the elevated plus maze (EPM) for Experimental 1. (D) Representative track plots of EPM exploration for Experimental 1 (top: control, bottom: ketone). (E-H) Quantification of c-Fos activation (ratio of c-Fos-positive to DAPI-positive cells) in Experimental 2 for the primary motor cortex (M1; E), arcuate nucleus of the hypothalamus (ARC; F), bed nucleus of the stria terminalis (BNST; G), and central nucleus of amygdala (CeA; H). (I) Schematic illustrating the regions of interest for c-Fos quantification. (K) Representative immunofluorescence images of c-Fos (red) and DAPI (blue) staining within the quantified brain regions. Scale bar, 50 μm. Data are presented as mean ± SEM. (n = 6–10 per group). Statistical significance is denoted as *p < 0.05, **p < 0.01, ***p < 0.001.

[#07]

Why Do We Sabotage Ourselves?: Social Evaluation, Interoception and Cultural Adaptation in Self-Handicapping

Kyunghwan Lee[1], Daeeun Kim[1,2], Jinhee Kim[1], Ravael Rajan[1], Hackjin Kim[1]

[1]School of Psychology, Korea University, Seoul, Korea
[2]Department of Psychology, Korea Army Academy at Yeongcheon

Self-handicapping refers to self-protective behaviors in which individuals strategically regulate performance conditions in anticipation of potential failure. Although previous studies have primarily relied on self-report questionnaires, relatively little research has directly examined self-handicapping behavior in experimentally controlled performance-selection contexts. The present research developed a behavioral paradigm to investigate self-handicapping under socially evaluative conditions and examined how interoceptive accuracy and cultural adaptation relate to such behavior. Across Studies 1 and 2, participants completed a task-selection paradigm in which task difficulty (Easy vs. Difficult) and social visibility of task difficulty (Open vs. Private) were manipulated. Participants tended to avoid easy tasks and select difficult tasks more frequently when task difficulty would be visible to others, suggesting strategic self-handicapping in socially evaluative contexts. In Study 2, higher interoceptive accuracy, measured using a heartbeat counting task, was associated with lower self-handicapping behavior. In addition, self-esteem significantly mediated the relationship between interoceptive accuracy and avoidance-oriented self-handicapping. Study 3 extended this paradigm to foreign participants from individualistic cultural backgrounds (United States, United Kingdom, Canada, and Australia) currently residing in Korea. Cultural adaptation was assessed using the Vancouver Index of Acculturation (VIA). Results showed that greater adaptation to Korean mainstream culture was associated with increased self-handicapping behavior. In particular, acculturation moderated the interaction between task difficulty and social visibility, suggesting that cultural adaptation may alter the interpersonal meaning assigned to socially evaluative situations, thereby influencing self-handicapping behavior. Together, these findings suggest that self-handicapping is not merely a stable personality tendency but may emerge from how individuals interpret and respond to socially evaluative threat across internal and sociocultural levels of processing.

[#08]

Altered Cortical Hierarchical Organization In ADHD

Seoah Lee[1], Bo-yong Park[1,2]

[1]Department of Brain and Cognitive Engineering, Korea University, Seoul, Korea
[2]Center for Neuroscience Imaging Research, Institute for Basic Science, Suwon, Korea

Attention-deficit/hyperactivity disorder (ADHD) is associated with widespread alterations in brain function. Although prior studies have identified regional cortical abnormalities in ADHD, their network-level organization and topological underpinnings remain poorly understood. To better understand the organization of brain function in ADHD and its underlying biological mechanisms, we analyzed functional magnetic resonance imaging data from individuals with ADHD using manifold learning approaches. By applying dimensionality reduction techniques, we estimated manifold eccentricity (ME), a measure reflecting the topological organization of functional connectivity manifolds. Significant alterations in ME were observed in the limbic and default mode networks in individuals with ADHD, and these alterations were associated with atypical patterns of modular segregation. By leveraging ME, we demonstrated that in ADHD, regions with higher ME were positioned farther from the connectome core and showed increased within-network hubness but reduced cross-network integration, indicating enhanced functional segregation.

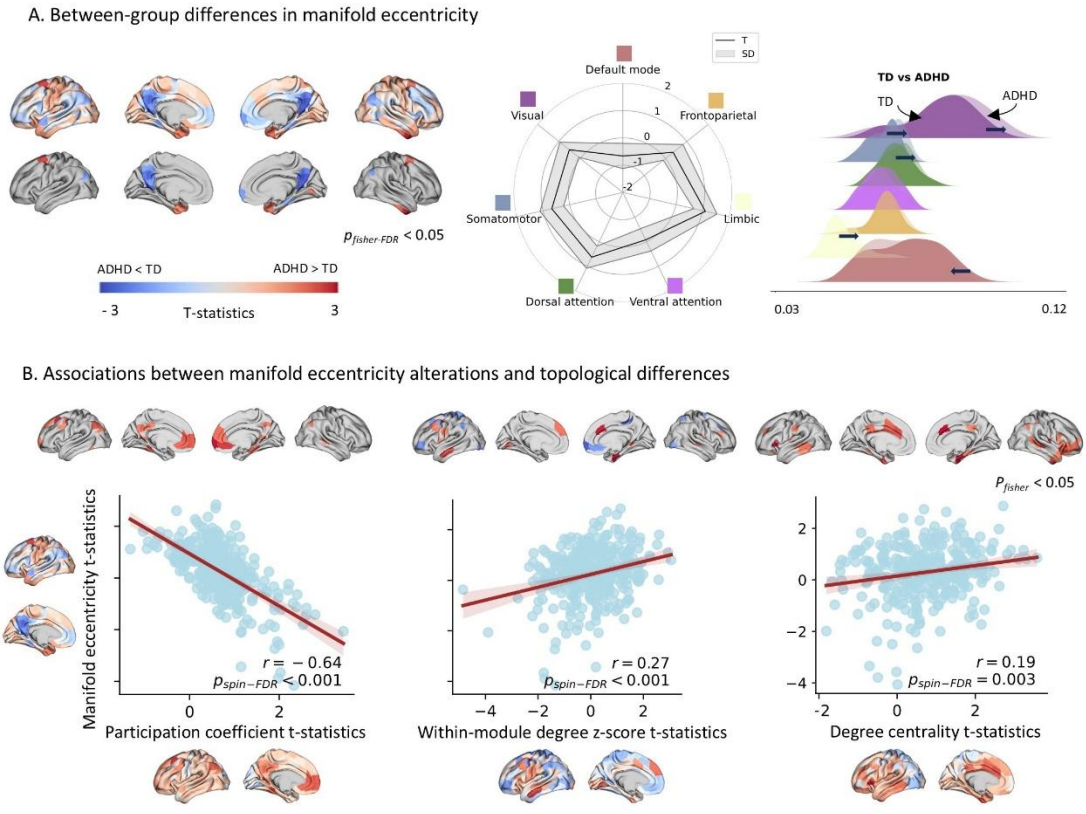

Figure 1. Between-group differences in ME and their associations with network topology measures.

[#09]

Multimodal fusion approaches for investigating discrete and continuous dimensions of Alzheimer's disease

Taeyeon Kim[1], Bo-yong Park[1,2]

[1]Department of Brain and Cognitive Engineering, Korea University, Seoul, Korea
[2]Center for Neuroscience Imaging Research, Institute for Basic Science, Suwon, Korea

Alzheimer's disease (AD) is a heterogeneous neurodegenerative disorder characterized by variability in clinical symptoms and disease progression. Conventional clustering approaches overlook individuals at the boundaries between disease states and fail to capture continuous patterns of disease progression. To address this limitation, we adopted a similarity network fusion (SNF) framework that integrates amyloid positron emission tomography (PET) centiloid, functional connectivity, and genetic information. After constructing patient-level SNF matrix, spectral clustering was applied and three subtypes, including CN-like, intermediate (MCI), and AD-like groups, were identified. The three subtypes exhibited significant differences across centiloid, functional connectivity, and genetic characteristics. These subtypes also showed distinct cognitive profiles that Cluster3 demonstrated significantly lower MMSE scores than Cluster1 and 2 (FDR < 0.001), suggesting a more advanced disease stage and supporting the clinical relevance of the subtype structure. Survival analysis based on the identified subtypes further revealed the steepest decline in survival probability in the AD-like Cluster3. Moreover, subjects ordered based on the principal component analysis-derived symptom severity axis exhibited trends consistent with standard disease progression. Our findings suggest that integrating multimodal brain and genetic data through SNF provides a powerful approach for uncovering clinically meaningful discrete and continuous patterns of AD progression.

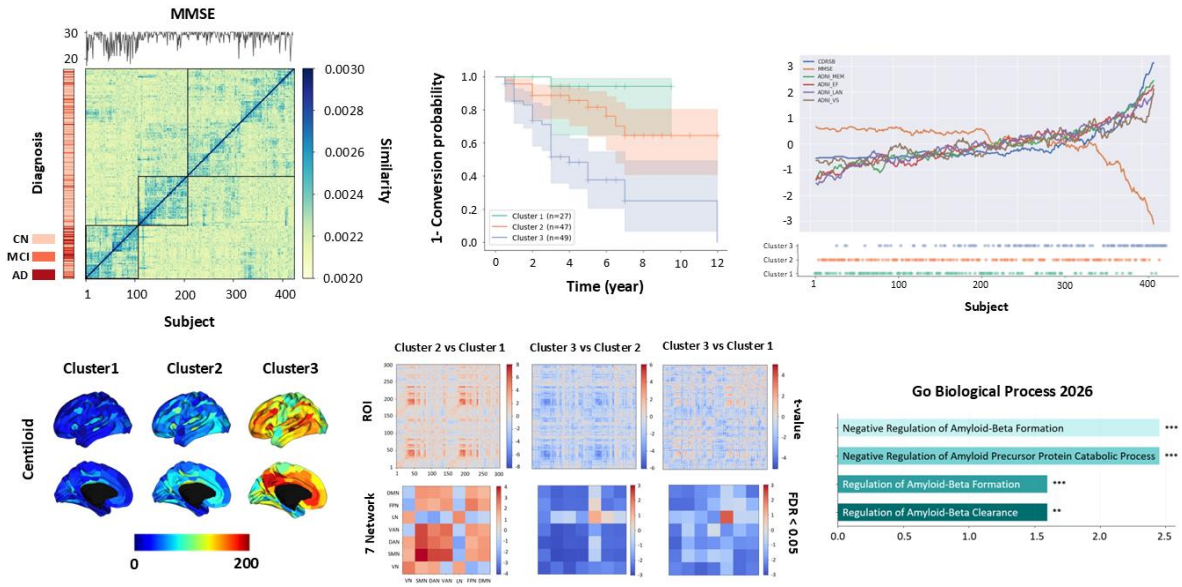

[#10]

Activation of Prefrontal SST Neurons Rescues the Immediate Extinction Deficit

Kyeong Im Jo, Seongmin Kwon, Yong Sang Jo, June-Seek Choi*

School of Psychology, Korea University, Seoul, Korea

Fear extinction is a key mechanism underlying exposure-based therapies for anxiety disorders and post-traumatic stress disorder (PTSD). Extinction training administered immediately after fear conditioning often produces impaired extinction memory, a phenomenon known as the Immediate Extinction Deficit (IED). However, most studies have examined IED using footshock-based paradigms, limiting our understanding of extinction processes under naturalistic threat conditions. To address this issue, we employed a predator-like chasing-robot paradigm and investigated how extinction timing influences extinction memory and prefrontal cortical function. SST-Cre mice received chemogenetic activation (hM3Dq) or inhibition (hM4Di) of somatostatin-expressing (SST) neurons in the medial prefrontal cortex. Fear-related behavior was assessed using a lever-press conditioned suppression task. Activation of SST neurons enhanced extinction memory following immediate extinction training, whereas inhibition of SST neurons impaired extinction retention. Notably, SST neuron activation rescued the immediate extinction deficit induced by predator-like threat conditioning. These findings indicate that SST neurons contribute to extinction memory formation, likely through regulation of prefrontal disinhibitory circuits. Together, our results demonstrate that extinction timing critically influences prefrontal inhibitory circuit function and identify SST neurons as a key neural substrate underlying extinction memory. Modulation of SST-mediated circuitry may represent a potential strategy for improving exposure-based treatments for trauma-related disorders.

Acknowledgements

This work was supported by the National Research Foundation of Korea (NRF) through grants funded by the Ministry of Science and ICT (MSIT, RS-2025-00517214) and by the Basic Science Research Program through the NRF funded by the Ministry of Education (NRF-2021R1A6A1A03045425).

[#11]

Object and Background contributions to neural representations in natural images

Suhyun Kim[1], Hojin Jang[1]

[1]Department of Brain and Cognitive Engineering, Korea University, Seoul, Korea

Scene understanding with objects and background is fundamental to human vision. Substantial evidence from cognitive neuroscience shows that objects and backgrounds are processed in partially distinct regions of the visual cortex, suggesting that they rely on different underlying representational mechanisms. Yet, real-world environments always contain objects embedded within backgrounds. Growing work reveals systematic, bidirectional influences between background and object processing, hinting at compositional integration rather than strict modularity. In this exploratory study, we investigate how object-derived and background-derived information jointly contribute to neural representations of complex natural images. Leveraging the large-scale Natural Scenes Dataset (NSD), we investigate whether brain activity patterns are better accounted for by an object-based representational strategy, defined by constituent objects and their relational structure, or by a background-based strategy that rapidly encodes global layout and scene-level structure. Applying representational similarity analysis across high-level visual cortex with each of the behavioral scene embeddings, we find that object-based embedding more strongly reflects the response structure in object-selective regions (FFA, EBA), whereas both strategies perform comparably in scene-selective regions (PPA, OPA), suggesting complementary contributions to scene understanding. We further compare human neural representational structure with convolutional neural networks that share an identical architecture but are trained to perform either object or scene categorization. While neural network features showed broadly similar patterns of representation prediction across visual regions, variance partitioning revealed lower shared variance between background and object representations in both networks. This dissociation suggests that although deep networks capture the overall representational geometry of the visual cortex, they have a different strategy to encode background and object information compared to humans. Taken together, our findings imply that object- and background-derived representations contribute complementarily to scene understanding in the human brain, especially at scene-selective regions. These patterns appear to differ from those observed in deep neural networks, pointing to potential differences in how human visual systems and artificial systems organize natural scene information.

[#12]

Associations of spatial gradients between magnetoencephalography and magnetic resonance imaging

Ju Hyung Lee[1], Bo-yong Park[1,2]

[1]Department of Brain and Cognitive Engineering, Korea University, Seoul, Korea
[2]BK21 Four Institute of Precision Public Health, Seoul, Republic of Korea

Gradient analysis, which estimates low-dimensional eigenvectors of connectivity, is widely used in recent neuroimaging studies to quantify the spatial organization of the human connectome [1]. While functional magnetic resonance imaging (fMRI) has been widely employed to investigate functional connectivity (FC) gradients, its low temporal resolution limited the ability to capture fine-grained temporal dynamics and micro-level neural processes [2]. In contrast, magnetoencephalography (MEG) offers superior temporal resolution compared to fMRI, allowing for the investigation of neural dynamics with greater temporal precision [3]. We hypothesized that gradients derived from MEG signals may better reflect neural-level connectome organization than those derived from fMRI. In this study, we explored the low-dimensional spatial organization of MEG-based functional connectomes, extending the concept of fMRI-derived gradients. Resting-state MEG, T1- and T2-weighted MRI, resting-state fMRI, and diffusion MRI data were obtained from the Human Connectome Project (HCP) (n = 89; mean ± standard deviation age = 28.60 ± 3.86 years; 47% females). Source-level MEG time series data were used to compute FC via amplitude envelope correlations. We focused on a wide frequency band (1.5–150 Hz), corresponding to the predefined frequency range provided in the HCP dataset [4]. Spatial gradients were then generated from the FC matrix using diffusion map embedding, and vertex-wise gradient values were summarized based on the Glasser atlas comprising 360 cortical parcels [5]. Functional and diffusion MRI data were preprocessed using the HCP minimal preprocessing pipelines [6], and the fMRI-based FC matrix was constructed using pairwise correlations of regional time series, while the diffusion MRI-based structural connectivity (SC) matrix was generated using probabilistic tractography. Additionally, the ratio between T1- and T2-weighting was calculated to estimate microstructural profile covariance (MPC) [7]. The correspondence between MEG-derived gradients and fMRI-FC, SC, and MPC gradients was evaluated using correlations with 1,000 spin permutation tests. Multiple comparisons were corrected using the false discovery rate (FDR) and Benjamini-Hochberg correction. Spatial correlations between MEG- and fMRI-FC-derived gradients revealed the strongest correlation for the second gradient, representing visual-somatomotor axis ($r = -0.674$, $p_{FDR} = 0.049$). Comparisons with MPC gradients showed a significant positive correlation for the first sensory-fugal gradient ($r = 0.615$, $p_{FDR} = 0.023$). Although correlations with SC gradients did not reach statistical significance ($p_{FDR} < 0.05$), a trend was observed for the second gradient of anterior-posterior axis ($r = 0.741$, $p_{FDR} = 0.081$). In this study, we identified spatial gradients of functional networks derived from resting-state MEG and validated their correspondence with gradients from multiple MRI modalities. Our findings suggest that MEG can effectively capture the structural-functional hierarchy of the human cortex.

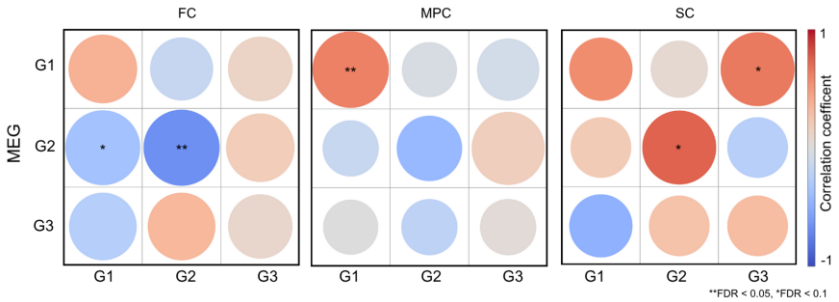

Figure 1. Associations between MEG and MRI gradients.

[#13]

The Role of Recurrent Connections in Holistic Face Processing

Jiwon Kim[1], Hojin Jang[1]

[1]Department of Brain and Cognitive Engineering, Korea University, Seoul, Republic of Korea

Holistic processing is a hallmark of human face recognition, yet its computational basis remains unclear. Recurrent processing, which is pervasive in the ventral visual pathway, may provide a neural substrate for transforming local facial information into holistic face representations. Here, we tested this hypothesis using recurrent convolutional neural networks equipped with lateral and top-down connections. Models were evaluated on three behavioral perturbation paradigms inspired by classic studies of face perception: random scrambling of local image patches, stimulus inversion, and misalignment of the upper and lower face halves. We quantified holistic processing as the performance cost induced by these manipulations, with larger impairments indicating stronger sensitivity to holistic facial structure. By this measure, recurrent models exhibited stronger holistic processing than purely feedforward models, with the effect increasing across recurrent timesteps. This pattern was more evident in models with lateral recurrence, and virtual cooling experiments confirmed that disrupting lateral rather than top-down connections produced the greater reduction in holistic processing. Attribution analyses further revealed that diagnostic features expanded over time, from initially local facial regions to broader spatial extents. Finally, the effects of recurrence were greater for familiar than unfamiliar faces, suggesting that prior experience may shape the emergence of holistic representations. Together, these findings suggest that recurrent connections, particularly lateral recurrence, may contribute to holistic face processing, with this contribution modulated by experience with individual faces.

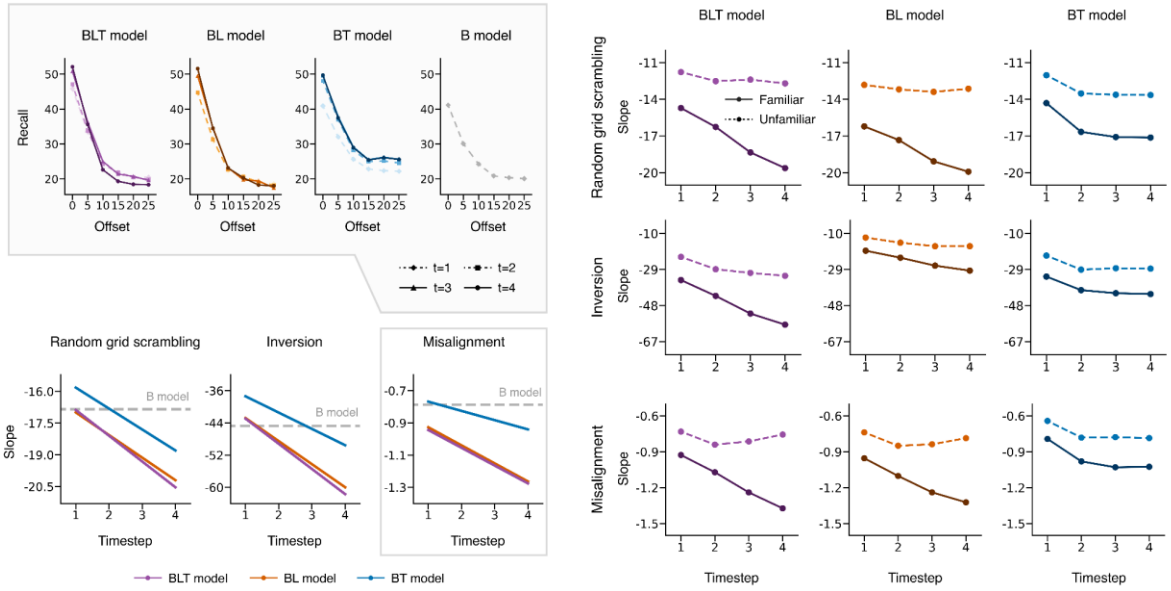

Figure 1. Behavioral comparison of feedforward and recurrent models across face-processing paradigms.

[#14]

Diagnosing Neural-Signal Dependence in Subject-General fMRI-to-Language Decoding

Sunghwan Lee[1], Jihun Kim[1], Chae Lynn Kim[1], Ji Yun Park[1], Jae-eon Kang[1], Jong-Hwan Lee[1]

[1]Deptartment of Brain and Cognitive Engineering, Korea University

Non-invasive fMRI-to-language decoders can generate fluent image descriptions from brain activity, but fluency alone does not establish that the generated language depends on measured neural signals. We evaluated subject-general fMRI-to-language decoding on the Natural Scenes Dataset using a leave-one-subject-out protocol. A decoder was trained with contrastive brain-representation alignment followed by supervised caption fine-tuning. After training, the checkpoint, prompt, decoding strategy, and evaluation pipeline were fixed, and only the test-time fMRI input or available voxel populations were manipulated. This design treated the decoder as a fixed analysis instrument for testing whether caption generation depends on intact voxel values, voxel-location correspondence, correct stimulus-response alignment, and functionally defined visual-cortical signals. We applied three complementary diagnostics. First, inference-time perturbation and substitution controls tested neural-signal dependence at the input level. Zero set all voxel values to zero, Shuffle permuted voxel values within each trial, Subject-mean replaced each trial with the subject-wise mean response, and same-subject Mismatch replaced the target trial with the response to a different stimulus from the same subject. Second, decoder-free fMRI-to-image retrieval tested whether frozen brain representations preserved stimulus identity by ranking a fixed gallery of unseen NSD test images. Third, ROI-based virtual lesioning tested anatomical selectivity by masking functionally defined visual-cortical regions, including ventral visual cortex, fLoc-places, PPA, OPA, fLoc-faces, FFA, and OFA. ROI effects were compared with size-matched random-contiguous control lesions within the subject-specific visual mask, and semantic-subset analyses tested whether lesion effects covaried with decoded content. The intact decoder achieved reliable held-out-subject captioning, establishing task-level utility. However, perturbation diagnostics showed that this utility depended strongly on matched fMRI input. In the benchmark-aligned S8 fold, CIDEr decreased from 26.57 under intact input to 8.08 under Subject-mean replacement, 5.93 under same-subject Mismatch, 6.19 under Shuffle, and 5.84 under Zero input. The Mismatch control was especially informative because it preserved realistic same-subject fMRI structure while breaking stimulus-response alignment, showing that realistic neural activity alone was insufficient unless it was matched to the correct stimulus. Representation-level retrieval provided convergent evidence that the aligned brain representation preserved stimulus identity. Intact fMRI embeddings retrieved the viewed image above chance from a 1,000-image gallery, whereas disrupted inputs collapsed to near chance. In the S8 fold, Real input achieved R@10 = 0.3062, whereas Shuffle and Zero were approximately 0.01. Across additional held-out subjects, Real input achieved R@10 = 0.4069 ± 0.0519, while disrupted inputs remained near chance. Virtual lesioning further revealed anatomically structured model-level dependence within visual cortex. Lesioning fLoc-places produced the largest caption degradation, reducing CIDEr by 34.8%, followed by PPA, FFA, and ventral visual cortex. These effects exceeded size-matched random-contiguous control lesions, indicating that the lesion profile was not explained by voxel count alone. Semantic-subset analyses showed that place-selective lesions most strongly affected place-related captions, whereas face-selective effects were weaker and more variable. Together, these results show that perturbation, retrieval, and virtual-lesion diagnostics can separate task-level captioning utility from model-level dependence on intact, stimulus-aligned, and anatomically structured fMRI signals.

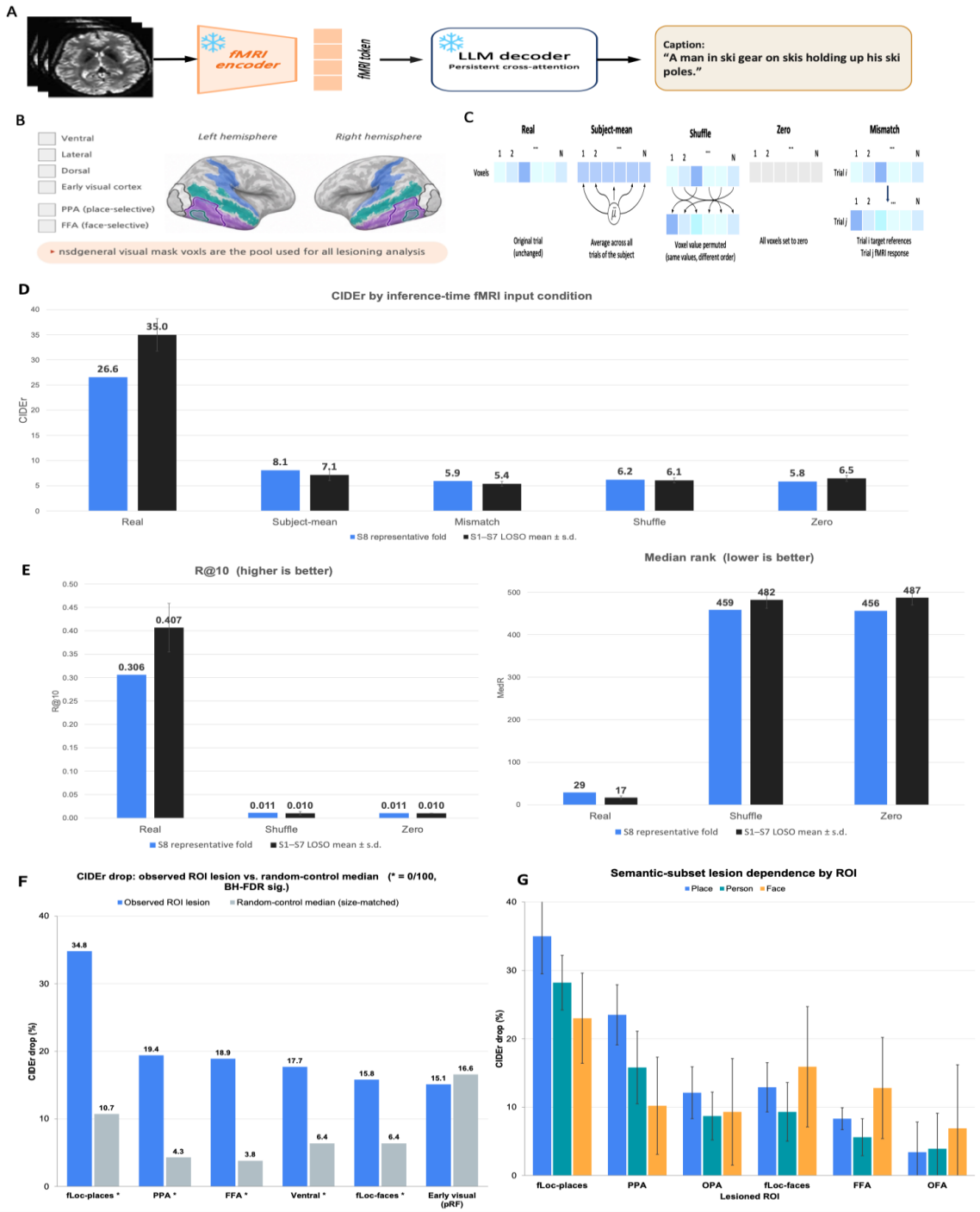

Figure 1. Diagnostic workflow for testing neural-signal dependence with results. a, A fixed fMRI-to-language decoder mapped fMRI responses to captions through brain-token conditioning and persistent cross-attention. b, Virtual lesioning targeted functionally defined visual-cortical ROIs within the subject-specific visual mask. c, Input perturbation and substitution controls tested dependence on intact voxel values, voxel-location correspondence, and stimulus-response alignment. d, Captioning performance dropped sharply when intact fMRI was replaced by Subject-mean, same-subject Mismatch, Shuffle, or Zero inputs. e, fMRI-to-image retrieval was above chance under intact input but collapsed to near chance under Shuffle and Zero controls, as shown by R@10 and median rank. f, ROI-based virtual lesioning showed stronger degradation for ventral and place-selective visual regions than for size-matched random-contiguous controls. g, Semantic-subset analyses indicated that lesion effects covaried with decoded content, especially for place-related captions.

[#15]

Whole-Brain Decoder-Based Real-Time fMRI Neurofeedback: Strengthening the Interoceptive Salience Network

Jihun Kim[1], Jae-eon Kang[1], Juyoung Kim[2], Yuri Kim[2], Hyojun Choi[2], Hackjin Kim[2†], Jong-Hwan Lee[1†]

[1]Department of Brain and Cognitive Engineering, Korea University, Seoul, Korea
[2]School of Psychology, Korea University, Seoul, Korea

Interoception is altered across psychiatric disorders yet trainable (Craig, 2002; Khalsa et al., 2018; Sugawara et al., 2020). We developed breath-focused whole-brain decoder neurofeedback, comparing real feedback (n=12) with yoked sham (n=8) across five days (Fig. 1A). Decoded BreathCounting probability rose from 0.37 to 0.73 without a comparable sham trend (Fig. 1B). Perturbation implicated insula, thalamus, brainstem, and cingulate regions (Fig. 1C); resting-state connectivity indicated salience-network integration (Fig. 1D), supporting ROI-free regulation of distributed interoceptive circuits.

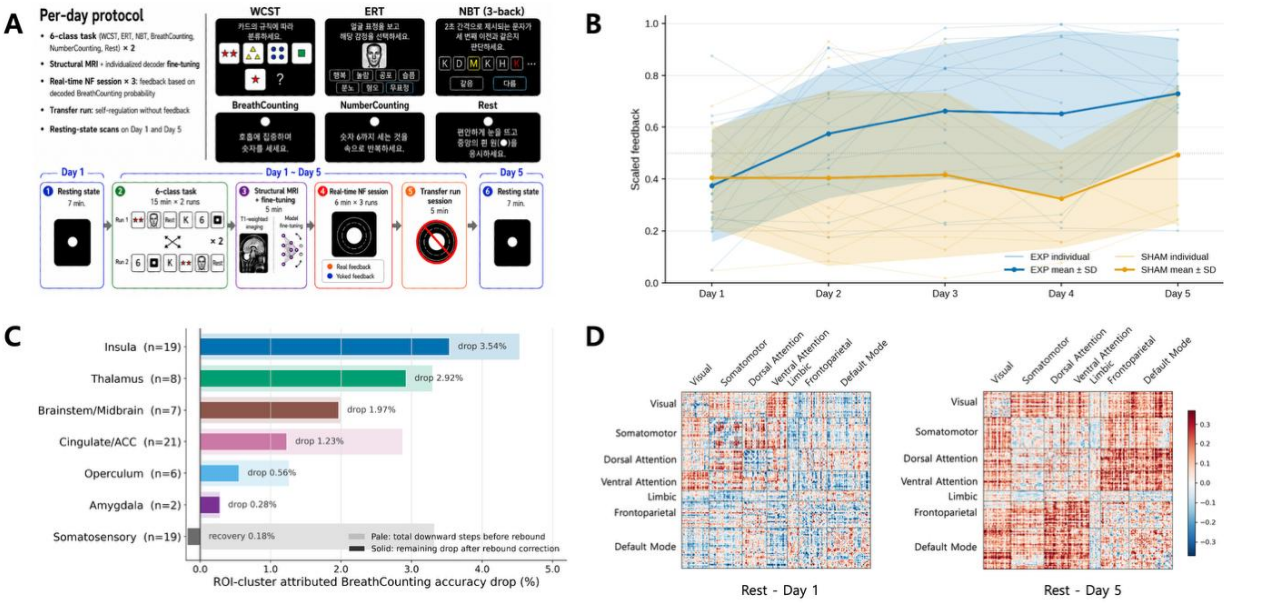

Figure 1. A: real-time fMRI Neurofeedback Task Pipeline, B: Daily Neurofeedback, mean (SD): exp vs sham, C: ROI-cluster decomposition of the masking-induced BreathCounting accuracy drop, D: Functional Connectivity Comparisons between exp and sham group

[#16]

State-dependent associations between perceptual dimensions of electric vehicle driving sounds and attentional response speed

Chaelynn Kim[1], Changha Lee[1], Jae-eon Kang[1], Minwoo Lee[1], Jong-Hwan Lee[1]

[1]Department of Brain and Cognitive Engineering, Korea University, Seoul, Korea

The transition to electric vehicles (EVs) has changed the in-cabin acoustic environment by reducing intrinsic powertrain noise and increasing the importance of intentionally designed driving sounds. Although EV sounds are commonly evaluated in terms of comfort, preference, and acoustic quality, their relevance to safety-related attentional performance may depend on the listener's momentary physiological state. This study examined whether perceptual dimensions of EV driving sounds are associated with reaction time (RT) during an attention task and whether these associations are moderated by ocular state. Forty-two healthy adults completed the Attention Network Test (ANT) under ten loudness-equalized EV driving-sound conditions while facial video was recorded using a front-facing webcam. Before the task, participants rated each sound using twelve bipolar adjective pairs, and the ratings were summarized by principal component analysis. Eye Aspect Ratio (EAR) was extracted from facial landmarks and normalized to each participant's baseline. Two pre-target ocular indicators were computed from a 900 ms window ending immediately before target onset: normalized median EAR, reflecting relative eye openness, and normalized EAR standard deviation (EAR SD), reflecting ocular instability. Log-transformed RT was analyzed using linear mixed-effects models with random intercepts for participant and participant-by-sound clusters. Model 1 tested main effects of task variables, sound dimensions, satisfaction, and EAR measures, whereas Model 2 tested interactions between sound dimensions and ocular instability. P-values were adjusted using the Benjamini-Hochberg false discovery rate procedure. The ANT manipulation produced the expected behavioral effects, with slower responses for incongruent trials and faster responses for spatial-cue trials. EAR-derived measures robustly predicted attentional performance. Greater normalized median EAR was associated with faster RTs (beta = -0.208, $p_{FDR} < 0.001$), whereas greater normalized EAR SD was associated with slower RTs (beta = 0.191, $p_{FDR} < 0.001$). The model also showed moderate out-of-sample generalizability in leave-one-subject-out validation (r = 0.519, RMSE = 0.191, MAE = 0.150), supporting that the observed associations were not limited to within-sample model fitting. Perceptual sound dimensions did not independently predict RT after correction. However, two dimensions interacted with ocular instability. Under high EAR SD, sounds perceived as more negative or tedious were associated with slower responses (Sound PC2 x EAR SD: beta = 0.059, $p_{FDR} = 0.041$), whereas colder-perceived sounds were associated with faster responses (Sound PC4 x EAR SD: beta = -0.063, $p_{FDR} = 0.038$). Sound PC2 mainly reflected evaluations such as boring, irritating, plain, and classic, while Sound PC4 was dominated by the warm-cold contrast. These findings suggest that the attentional relevance of EV driving sounds is state-dependent rather than fixed. For EV sound design, subjective preference alone may be insufficient; camera-based indicators of vigilance should also be considered when evaluating in-cabin sounds for safety-relevant responsiveness.

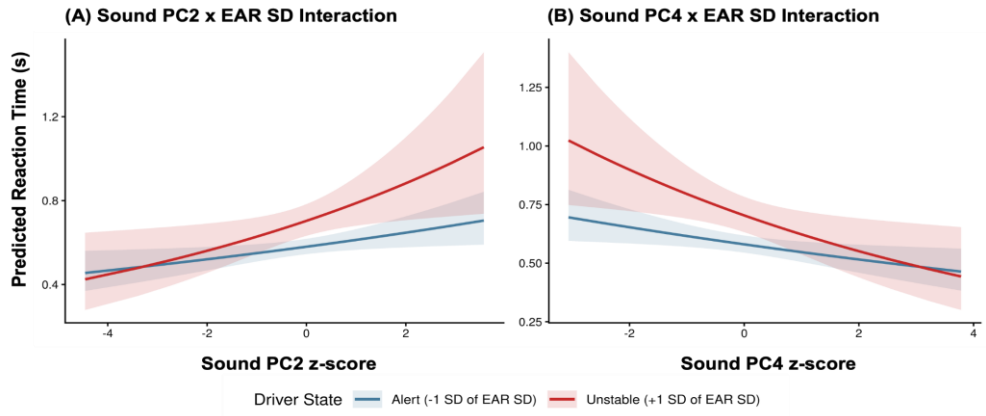

Figure 1. Interaction between perceptual sound dimensions and ocular instability.

[#17]

Differences in HRV Across Task Types During Home-Based Introceptive Training

Joungwoo Choi[1], Minwoo Lee[1], Chaelynn Kim[1], Jong-Hwan Lee[1]

[1]Department of Brain and Cognitive Engineering, Korea University, Seoul, Korea

Adolescent mental health problems require preventive approaches before symptoms become clinically severe. Interoception, the sensing and interpretation of internal bodily signals, links mental states with measurable physiological regulation. Among interoceptive signals, respiration is well suited for training because it can be voluntarily attended to and regulated and is reflected in physiological recordings. This pilot study examined whether home-based, breath-focused interoceptive attention training in early adolescents could be evaluated using repeated single-lead ECG and heart rate variability (HRV) analysis. This analysis used ECG data from the BBMI study, a pilot project for interoception training. Participants completed ~10-min home training sessions using a smartphone application and a chest-worn Movesense HR+ sensor (BLE, 200 Hz). Of 13 participants, 11 with identifiable task labels were included. In each session, participants performed one of two tasks. In the Breath Counting Task (BCT), participants counted their own breaths while maintaining slow nasal breathing with the mouth closed. In the Number Counting Task (NCT), participants counted randomly presented numbers without explicit breath regulation, serving as a non-breath-focused control. The dataset included fixed-task groups and a within-subject group with session-wise random task assignment. A total of 346 ECG sessions were processed. ECG signals were preprocessed to reduce spike artifacts and improve R-peak reliability. After excluding the initial 5-s stabilization period, the session-wise absolute 99th percentile defined a ±4×P99 clipping threshold. Signals were band-pass filtered at 0.5–40 Hz, and R peaks were detected using NeuroKit2. Beats containing clipped samples within ±100 ms of the R peak were flagged as unreliable. RR intervals outside the physiological range, deviating from the local median, or adjacent to spike-contaminated beats were removed. After session-level quality control, 343 sessions were included. Parasympathetic and short-term HRV indices showed little difference between tasks: RMSSD ($d = -0.19$), pNN50 ($d = -0.13$), and HF power ($d = +0.06$). In contrast, overall variability and slow-oscillation-related indices were higher in BCT. SDNN was 57.0 ms in BCT and 43.7 ms in NCT ($d = -0.73$), and LF/HF was 9.5 vs. 3.2 ($d = -1.05$; all $p < .001$). Nonlinear analysis showed a similar pattern: SD1 was nearly identical, whereas SD2 was larger in BCT (79.8 vs. 59.1 ms, $d = -0.74$, $p < .001$). This SD2 difference converged in both between-subject and within-subject comparisons. Post-training arousal also tended to decrease more after BCT. These findings indicate that home-based ECG can capture task-related physiological signatures during interoceptive training. The HRV differences are best interpreted as respiratory influences associated with slow breath-focused performance, not direct evidence of parasympathetic enhancement. Larger multimodal analyses integrating ECG, IMU, video, and surveys are needed to evaluate mental-health relevance.

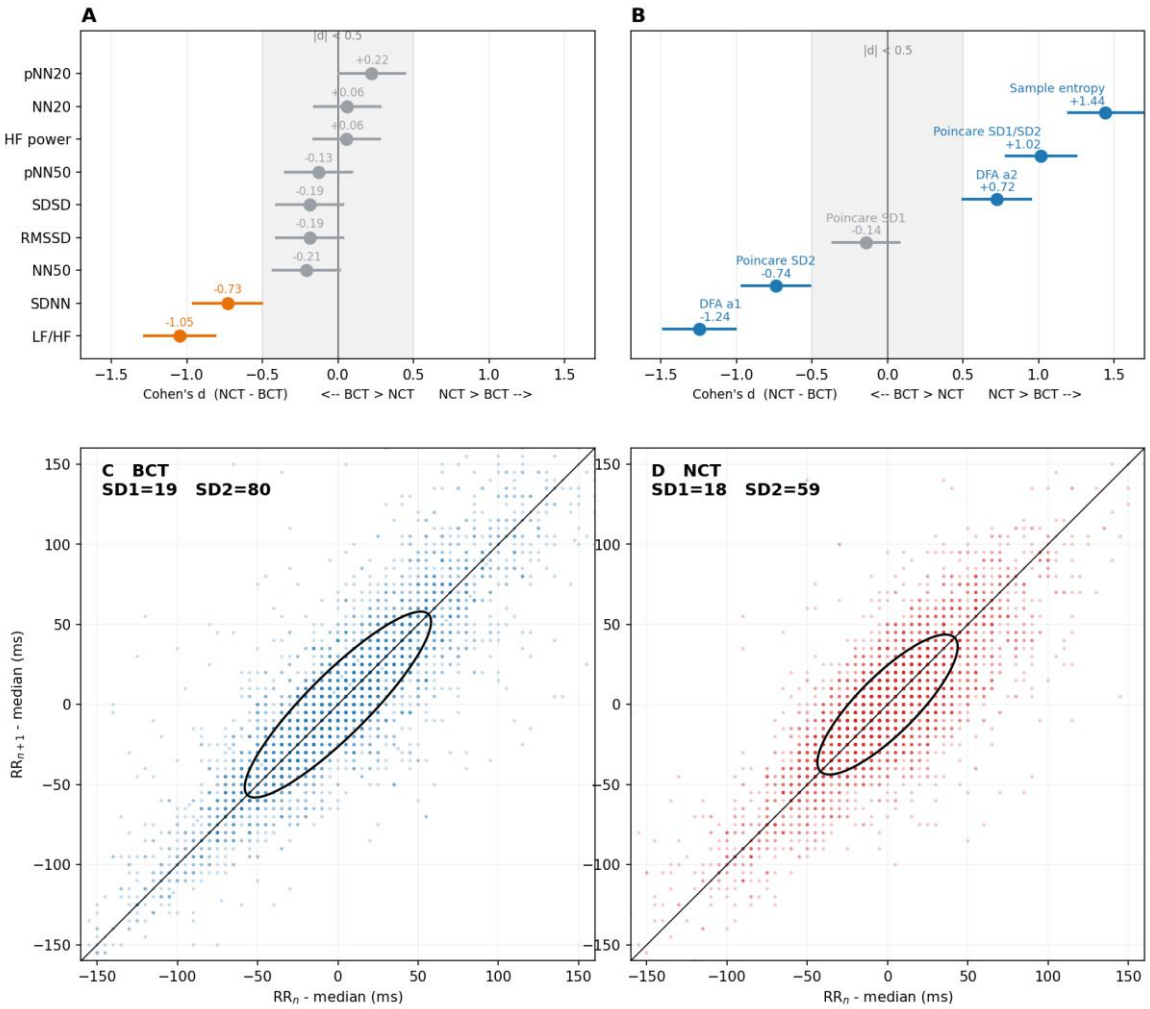

Figure 1. HRV feature differences by task type. A. Time- and frequency-domain HRV features. B. Nonlinear HRV features. C,D. Representative Poincare plots for BCT and NCT.

[#18]

The Priming Effect of the Korean Adnominal Transformation Suffix "-ㄴ" in Phrase Parsing: A Lexical Decision Task Study

Taeryung Kim[1], Kichun Nam[2]†

[1]Department of Linguistics, Korea University, Seoul, Korea
[2]School of Psychology, Korea University, Seoul, Korea
† Corresponding Author: kichun@korea.ac.kr

Korean sentences are structured around syntactic units called "Eojeol"s, unlike English and other isolating languages where syntactic roles are largely determined by word order. Eojeols are formed by attaching case markers or derivational/inflectional suffixes to stems. This study investigates whether the Korean adnominal transformational suffix (관형사형 전성어미) "-ㄴ" functions as a critical structural cue for phrase parsing and construction. We hypothesized that the presence of "-ㄴ" in a prime stimulus would facilitate the processing of a subsequent target stimulus by signaling upcoming phrase formation, regardless of whether the prime itself is a real word or a nonword. A visual Lexical Decision Task (LDT) was conducted with 40 native Korean speakers. After removing outliers and participants who misunderstood the task instructions based on a 2.5 standard deviation (SD) threshold, data from 38 participants were utilized for the final statistical analysis (n = 37for descriptive reporting). The experiment employed a 2 x 2 within-subject design with four primary conditions crossing Prime Attribute (Word vs Nonword) and Target Attribute (Word vs Nonword), creating 4 conditions of (1) word + word, (2) word + nonword, (3) nonword + word, (4) nonword + nonword. Primes consisted of words or phonologically permissible nonword sending with the adnominal suffix '-ㄴ'. Targets consisted of words or nonwords attached with the nominative case marker '-이/가'. All lexical items were controlled for word frequency (4.5 < Zipf < 5.5) and syllable length. Linear Mixed-Effects (LME) model analysis revealed a statistically significant priming effect. When the target stimulus was a real word, reaction times (RT) were significantly faster regardless of the lexical status of the prime (606.6 ms for the Word-Word condition vs. 614.9 ms for the Nonword-Word condition). Furthermore, accuracy rates (ACC) reached their highest in the Word-Word condition (96.3%). These findings indicate that the adnominal suffix '-ㄴ' independently exerts a strong structural facilitation effect during online sentence processing, acting as an implicit parser that prepares the cognitive system for subsequent phrasal integration. This suggests that morphosyntactic markers in Korean play an autonomous role in incremental structural parsing, independent of lexical-semantic activation.

[#19]

Investigation of the Mechanisms of Cross-Modal Congruency Sequence Effect: A Diffusion Model Analysis

Jin Ho Kim[1], Yang Seok Cho[1]

[1]School of Psychology, Korea University, Seoul, Korea

The congruency sequence effect (CSE) refers to the reduction in the congruency effect following an incongruent trial compared with the effect following a congruent trial. Although this CSE has been shown to transfer across different sensory modalities, the mechanisms underlying this cross-modal transfer remain unclear. To investigate these mechanisms, we applied the diffusion model for conflict tasks (DMC) and examined parameter modulations across four cross-modal conflict tasks. The amplitude parameter A, which represents the strength of automatic activation elicited by task-irrelevant information, showed a marginal tendency to be smaller following an incongruent trial than following a congruent trial. In contrast, the controlled drift rate (μc), which reflects the rate of task-relevant evidence accumulation, showed no such modulation. Importantly, these parameter modulations were absent when the cross-modal CSE was not observed. The reduction in parameter A following incongruent trials suggests that the cross-modal CSE reflects inhibitory control, while the lack of modulation in parameter μc cannot be explained by bottom-up priming effects. These findings support the view that the cross-modal CSE is a product of cognitive control, and that this control operates through an inhibitory mechanism on the task-irrelevant dimension.

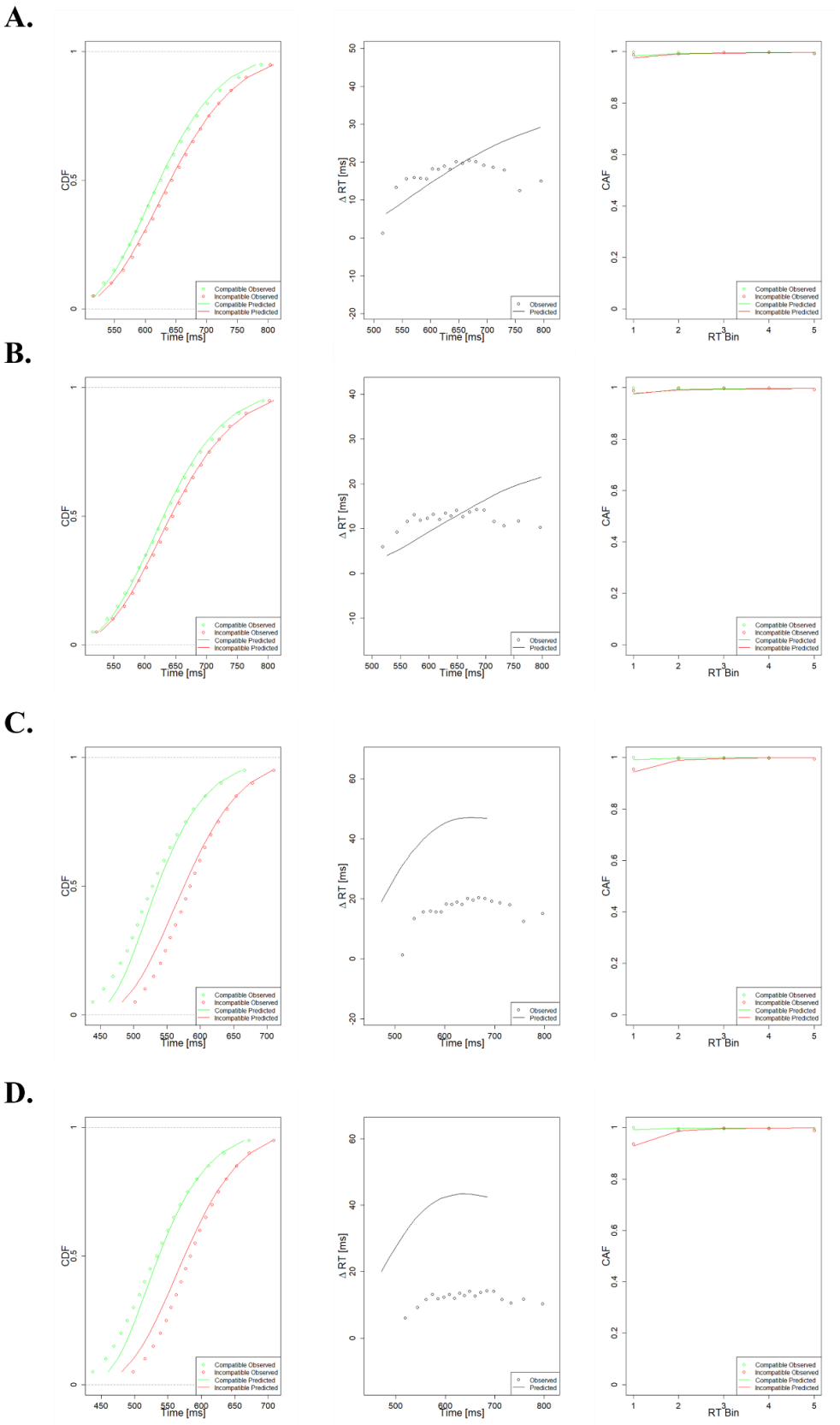

Figure 1. CDF, Delta plots, and CAF for Experiment 1.

[#20]

Decoding Visual Event Captions from 7T Naturalistic Movie-watching Brain via 4D fMRI Encoding and Persistent Cross-Attention

Ji-Yun Park[1], Sung-Hwan Lee[1], Ji-Hun Kim[1], Chae-Lin Kim[1], Jong-Hwan Lee[1]

[1]Department of Brain and Cognitive Engineering, Korea University, Seoul, Korea

Reconstructing the semantic content of perception from brain activity is a central goal of neural decoding, yet most fMRI-to-language models have been developed on static-image viewing rather than on the continuous, dynamic input that characterizes natural vision. We propose BIT-LLM-Video, a framework that decodes short visual-event captions from 7T naturalistic movie-watching fMRI in the HCP Young Adult cohort. Movie clips are segmented into non-overlapping visual-event intervals, each paired with a fMRI window and a canonical one-sentence caption describing the people, objects, scene context, actions, and interactions in view. A SwiFT-based 4D encoder, initialized by masked spatiotemporal BOLD reconstruction, converts each movie-evoked BOLD window into a sequence of brain tokens, which are then aligned with frozen video and caption-text representations in a shared CLIP-style embedding space through a tri-modal (fMRI–video–text) contrastive objective. For generation, the brain tokens are attached to a frozen instruction-tuned LLM as a persistent key–value memory that the decoder re-attends to across multiple layers during autoregressive decoding, so that neural evidence stays accessible throughout instead of being supplied only once as a prefix. During this stage, only the projector and the cross-attention adapters are trained. As an initial step, we characterized the decoding targets: segmenting four HCP 7T movie runs with TransNet V2 and merging shots into units of at least 3 s yielded 543 visual-event segments (mean duration 6.7 ± 5.1 s; median 5.0 s), setting the encoder window near 12 TRs (TR = 1 s). After training, the decoder will be evaluated under a subject-heldout protocol with standard captioning metrics (BLEU, ROUGE-L, METEOR, CIDEr, SPICE) and BERTScore, together with neural-grounding controls (zeroed and intra-window-shuffled inputs, prefix versus persistent conditioning) and pretraining-objective ablations. By pairing a volumetric 4D encoder with this persistent interface, the framework extends image-based brain captioning toward dynamic naturalistic visual events while preserving explicit neural grounding.

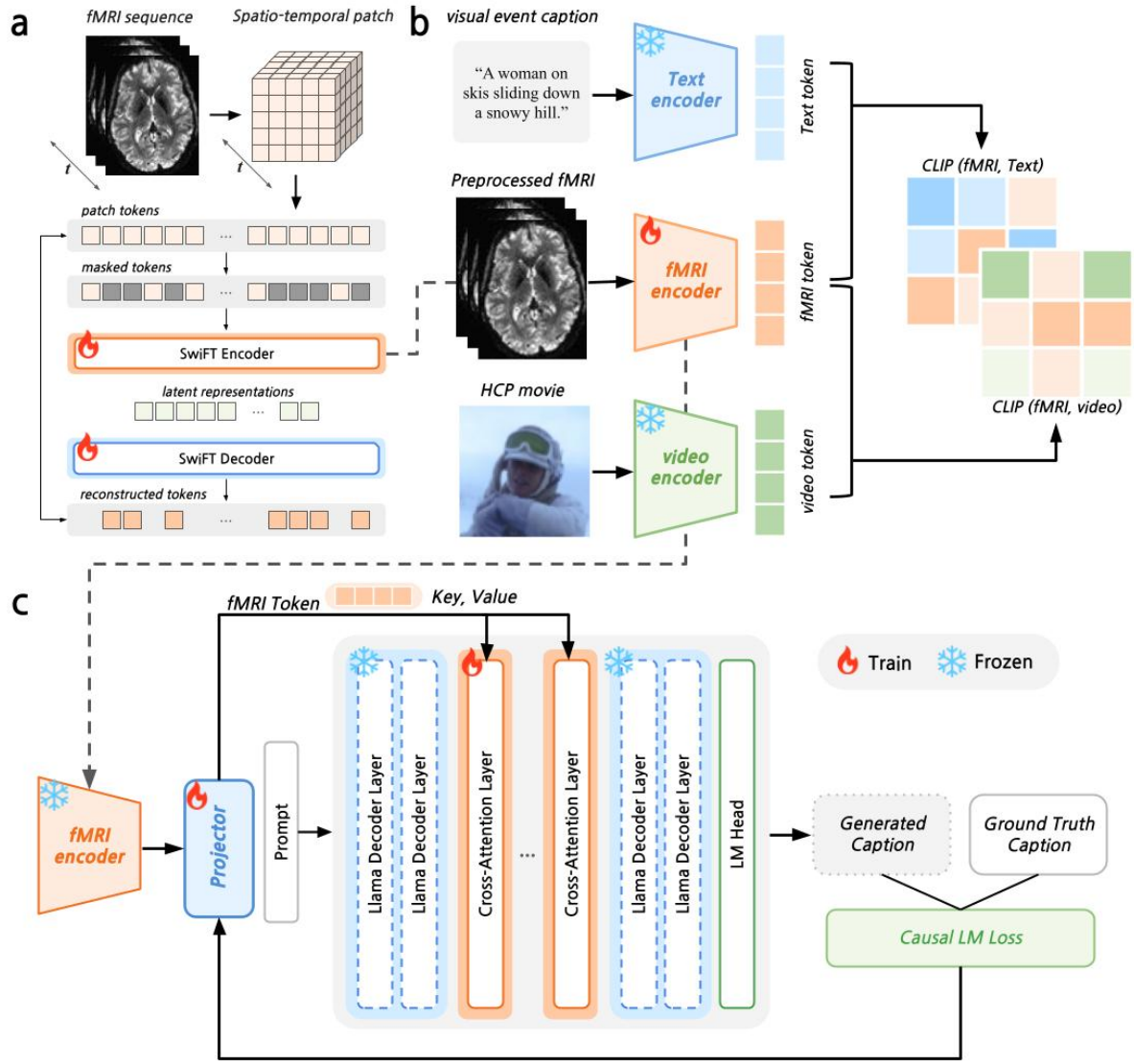

Figure 1. The BIT-LLM-Video training framework. (a) Self-supervised MAE pre-training: masked spatio-temporal fMRI patch tokens are encoded by the SwiFT encoder and reconstructed by a decoder. (b) Tri-modal alignment: the fMRI encoder is aligned with frozen text and video encoders in a shared CLIP space, with caption text. (c) Supervised fine-tuning: the frozen fMRI encoder feeds a trainable projector and interleaved cross-attention layers that expose brain tokens as a persistent key–value memory to a frozen Llama backbone.

[#21]

Preliminary Physiological and Resting-State Connectivity Trends During Interoceptive Neurofeedback Training

Jae-eon Kang [1], Jihun Kim [1], Hyojun Choi [2], Yuri Kim [2], Juyoung Kim [2], Hackjin Kim [2], Jong-Hwan Lee [1]

[1]Department of Brain and Cognitive Engineering, Korea University, Seoul, Korea
[2]School of Psychology, Korea University, Seoul, Korea

Interoceptive regulation involves coordinated changes in brain and body signals, yet breath-focused neurofeedback studies must distinguish meaningful autonomic regulation from physiological influences on BOLD connectivity. We conducted an interim paired analysis of a 5-day controlled, yoked-sham real-time fMRI neurofeedback study targeting breath-focused interoception. The current sample included six completed experimental–sham pairs, yielding 12 healthy adult participants. The experimental group received contingent feedback based on the online output of a whole-brain decoder estimating breath-counting-related interoceptive brain-state expression, whereas yoked sham participants received matched non-contingent feedback from the corresponding experimental participant's day and run. We examined Day 1 to Day 5 changes in resting physiology and resting-state functional connectivity across multiple denoising branches. Physiology-aware preprocessing progressively reduced BOLD–physiology coupling, with the full RETROICOR+RVT+HR branch showing the lowest residual coupling. Under full physiological denoising, the experimental group showed greater increases in mPFC-dlPFC connectivity and Salience-FPN connectivity relative to yoked sham controls, while anterior-insula-dlPFC connectivity showed a similar but non-significant trend. Across individuals, larger reductions in resting heart rate and greater mPFC-dlPFC connectivity increases were associated with better transfer performance. Baseline interoceptive awareness further appeared to scale connectivity plasticity, with higher K-MAIA and MAIA body-awareness scores predicting larger changes in salience-network-related connectivity. These interim findings suggest that whole-brain decoder-based breath-focused neurofeedback may engage autonomic regulation and prefrontal control mechanisms, while highlighting the importance of physiology-aware analysis for interpreting resting-state connectivity changes in interoceptive neurofeedback. Larger samples and physiology-adjusted models are needed to confirm the neural and physiological mechanisms of training.

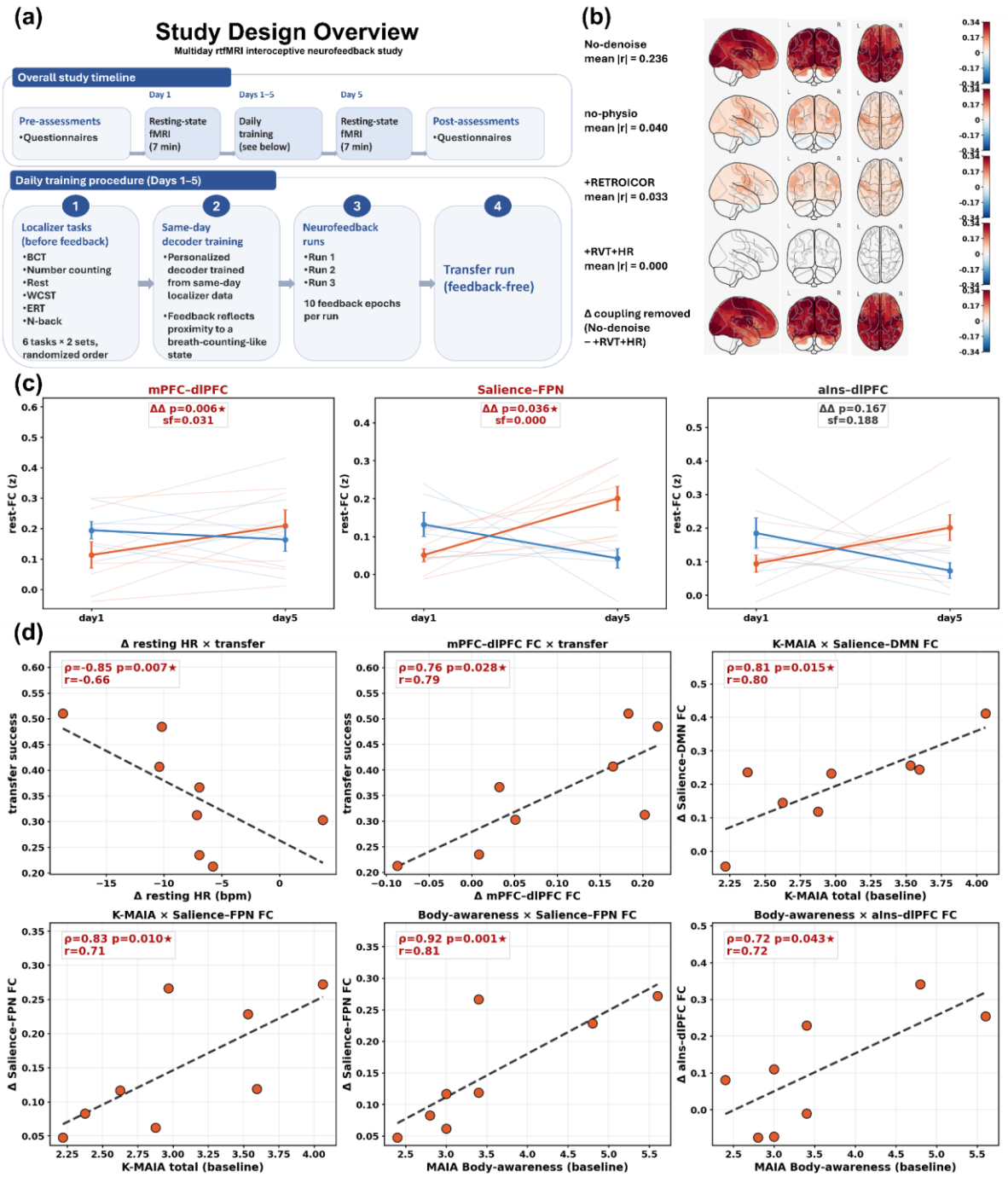

Figure 1. Overview of the neurofeedback protocol and main findings.

[#22]

Heartbeat-Evoked Potentials Across Interoceptive, Resting and Diverse Cognitive States: An EEG-fMRI Study

Changha Lee[1], Jong-Hwan Lee[1]

[1]Department of Brain and Cognitive Engineering, Korea University, Seoul, Korea

Interoception is the ability to perceive internal bodily signals involving various mental processes, gaining significant attention due to its crucial role in cognitive, psychiatric traits, and emotional processing. Heartbeat-evoked potentials (HEPs), computed as a grand average of heartbeat time-locked potentials, serve as a key measure to evaluate interoception utilizing EEG. Although limited studies have investigated HEPs in simultaneous EEG-fMRI environments, leveraging this multimodal approach enables the concurrent investigation of both spatiotemporal dynamics and underlying neural substrates. Here, we utilized a respiratory interoceptive task to investigate differences in HEPs compared to resting-state and mind-wandering conditions. Additionally, three cognitive tasks—the Emotion Recognition Task (ERT), Wisconsin Card Sorting Task (WCST), and N-back task (NBT) were employed to explore how HEPs modulate depending on the demands of exteroceptive awareness. A total of sixty participants were recruited for the simultaneous EEG-fMRI experiment, and data from fifty-three participants were ultimately analyzed following the exclusion of seven low-quality datasets. Imaging was performed on a 3-Tesla Siemens Tim-Trio scanner with a 12-channel head coil, coupled with an MR-compatible BrainAmp MR system and a BrainCap MR containing 31 EEG electrodes and a single ECG channel. All EEG channels followed the international 10-20 system with the FCz channel as the reference, maintaining impedances below 10 kΩ at a 10 kHz sampling rate. Non-real-time sessions from a previous study were utilized, comprising two EEG-fMRI runs with three-minute blocks of either mindfulness (MF) or mind-wandering (MW). During MF blocks, participants focused on their natural breathing, while during MW blocks, they engaged in free thought. The administration order of MF/MW runs, Rest blocks, and cognitive tasks was pseudo-randomized and counterbalanced. For simultaneous data preprocessing, gradient and ballistocardiogram artifacts were minimized using average artifact subtraction and the optimal basis set method, with residual artifacts removed via independent component analysis (ICA). Utilizing ECG data from an electrode on the left back, R-peaks were detected using the fMRIB toolbox's 'fmrib_qrsdetect' function and manually inspected. Baseline correction of the HEPs was executed by generating pseudo-trial HEPs via 200 iterations of averaging randomized R-peak onsets, matching the trial count of real data, which were then subtracted from the real HEPs to yield pseudo-trial corrected HEPs. Statistical analysis was performed using one-way ANOVA with FDR corrections, followed by post-hoc t-tests on significant time points. Significant main effects were observed across several channels, particularly in the FC2 channel and the right parietal region channels, including T8, CP6, P4, P8, and TP10. Post-hoc t-tests further delineated specific conditional differences. Within the FC2 channel, the Rest and MW conditions exhibited significantly lower amplitudes compared to the other four conditions within the 376–388 ms time window ($p < 0.01$). Concurrently, in the right parietal regions, the MF condition elicited the highest amplitude relative to all other conditions. Notably, within the 280–348 ms window, the three external cognitive task conditions demonstrated negative amplitudes, whereas the Rest and MW conditions maintained amplitudes near 1 μV.

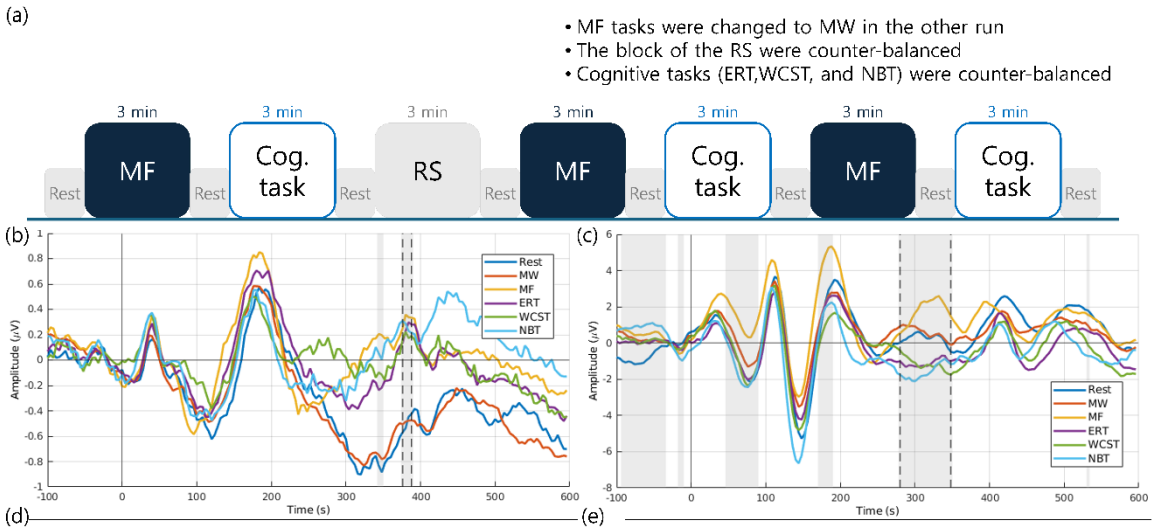

(d)

	Mean	STD	Rest	MW	MF	ERT	WCST
Rest	-0.4943	1.1849					
MW	-0.4860	1.3771	0.9718				
MF	0.3203	1.2898	**0.0030****	**0.0012****			
ERT	0.2352	1.2361	**0.0029****	**0.0063****	0.7333		
WCST	0.1876	1.1712	**0.0041****	**0.0089****	0.5865	0.8506	
NBT	0.2603	1.3602	**0.0033****	**0.0068****	0.8185	0.9008	0.7919

(e)

	Mean	STD	Rest	MW	MF	ERT	WCST
Rest	0.2571	3.8783					
MW	0.5810	2.4126	0.5917				
MF	1.7947	3.1713	**0.0296***	**0.0140***			
ERT	-1.0959	3.0735	0.0534	**0.0026****	**0.00001*****		
WCST	-1.1754	4.1635	0.0736	**0.0097****	**0.00009*****	0.9147	
NBT	-1.5887	4.3898	**0.0257***	**0.0023****	**0.00002*****	0.5285	0.6492

Figure 1. Experiment design and heartbeat evoked potential (HEP) results. (a) Experimental paradigm of the study. The order of the Resting State (RS) blocks and cognitive tasks (ERT, WCST, and NBT) was pseudo-randomized and counterbalanced, with cognitive tasks always following either MF or MW blocks. (MF: Mindfulness, MW: Mind-wandering, RS: Resting state). (b) HEP waveforms in the FC2 channel, with the shaded dashed region indicating the significant time window of 376–388 ms. (c) HEP waveforms in the right parietal region (averaged across T8, CP6, P4, P8, and TP10 channels), with the shaded dashed region highlighting the significant window of 280–348 ms. (d, e)Post-hoc pair-wise t-test matrices and descriptive statistics (Mean and STD) of the averaged HEP amplitudes calculated within the respective significant time windows for the (d) FC2 channel and (e) right parietal region. Asterisks indicate statistical significance (* *p<0.05, **p<0.01, ***p<0.001*)

[#23]

Behavioral Assessment Identifies Line-Dependent Susceptibility to Novelty-Induced Memory Enhancement

Eunjin Paek[1], June-seek Choi[1]

[1]School of Psychology, Korea University, Seoul, Korea

Memory is dynamically modulated by events occurring around the time of learning. The behavioral tagging hypothesis proposes that exposure to a novel experience within a critical temporal window can enhance the consolidation of otherwise weak memories. The present study examined whether novelty-induced memory enhancement differs across commonly used Cre-driver mouse lines. We compared spatial object recognition memory in three Cre-driver mouse lines bred on the same C57BL/6J genetic background (Pdyn-Cre/Cre, CRH-Cre/Cre, and SST-Cre/Cre). Mice were assigned to either a control group or a behavioral tagging group (brief exposure to a novel environment 1 hour before training). Preliminary analyses suggest that novelty exposure prior to training enhances memory retention after 24 hours in Pdyn-Cre/Cre mice ($t(11)=2.322$, $p=0.040$). However, this effect was not observed across other mouse lines. Behavioral characterization revealed significant line-dependent differences in exploratory behavior and locomotor activity during training. Pdyn-Cre/Cre mice exhibited greater object exploration than CRH-Cre/Cre mice ($t(20)=2.332$, $p=0.030$). In addition, locomotor activity differed significantly among mouse lines (one-way ANOVA, $F(2,28)=6.735$, $p=0.004$). Post hoc Dunnett's tests showed that SST-Cre/Cre mice displayed higher locomotor activity than both Pdyn-Cre/Cre ($p=0.022$) and CRH-Cre/Cre mice ($p=0.003$). These results indicate that the degree of novelty-induced memory enhancement varies considerably among Cre-driver mouse lines. Differences in baseline exploratory behavior and locomotor activity may partially account for this heterogeneity and should be taken into consideration when choosing behavioral paradigms for evaluating memory enhancement. More generally, the findings underscore the necessity of establishing baseline behavioral profiles in transgenic mouse lines prior to drawing conclusions about experimental manipulations.

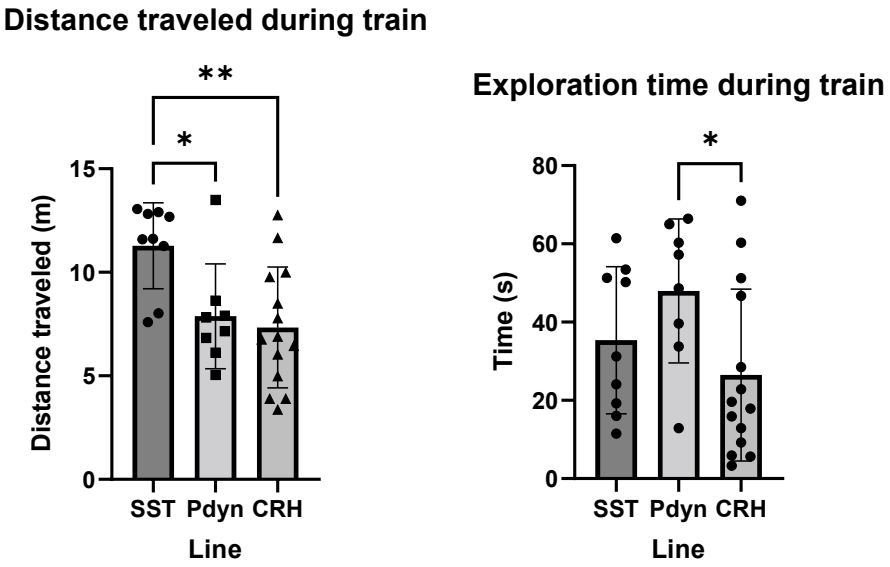

Figure 1. Title. Total locomotion and object exploration during train.

[#24]

VTA-to-CeA Dopamine Release Is Linked to Appropriate Action Selection During Active Avoidance

Eunsol Cho[1], Yong Sang Jo[1†]

[1]Department of Psychology, Korea University, Seoul, Korea

Active avoidance behavior enables individuals to predict and mitigate threats, playing a critical role in survival. While dopamine signaling is widely linked to active avoidance, its specific role within the central amygdala (CeA) remains poorly understood. To address this, we investigated the function of CeA dopamine signaling. Fiber photometry recording revealed that CeA dopamine release is modulated by both appetitive and aversive stimuli, responding to both conditioned (CS) and unconditioned stimuli (US). Notably, in trials where animals successfully performed avoidance behavior, CeA dopamine activity surged markedly during CS presentation compared to other behavioral outcomes. Conversely, failed avoidance trials exhibited minimal dopamine activation during the CS period. Importantly, these dynamic shifts in dopamine signaling correlated more strongly with the specific behavioral response than with the progression of training. These findings implicate that dopamine release in the CeA plays a role in action selection following CS presentation during active avoidance.

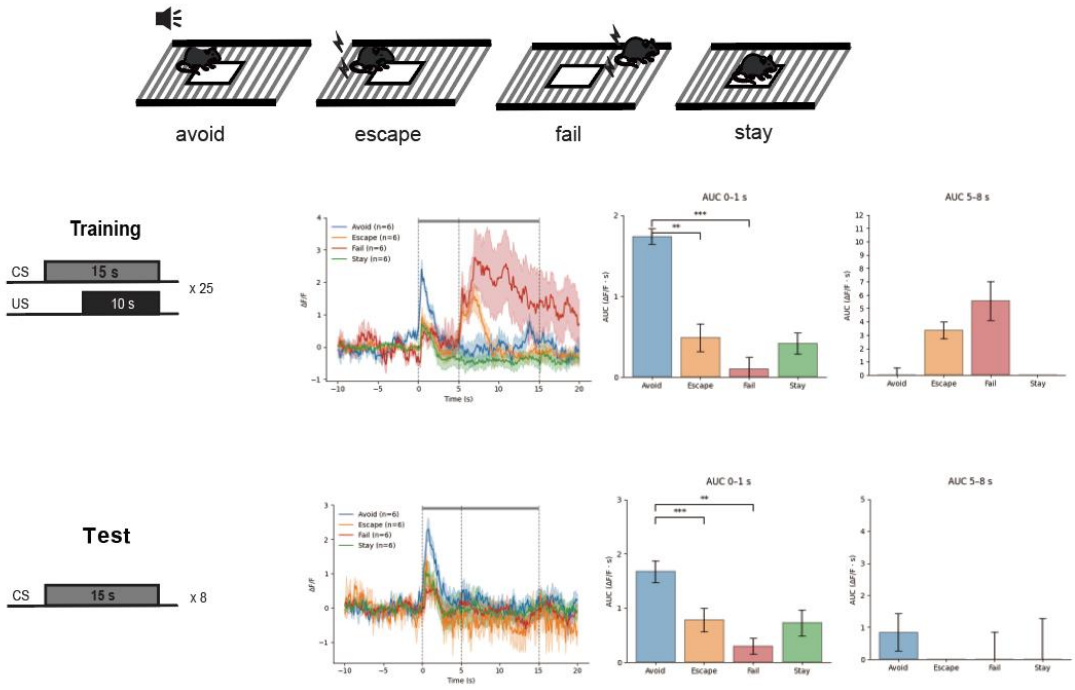

Figure 1. Enhanced CS-evoked CeA dopamine activity during successful avoidance behavior.

[#25]

Behavioral and Electrophysiological Evidence for Early Suppression of Singleton Distractors

Si Eun Choi[1], Jaein Lee[1], Yang Seok Cho[1†],

[1]Department of Psychology, Korea University, Seoul, Korea

We investigated feature-based distractor suppression using behavioral measures and EEG decoding. During EEG recording, participants searched for a target circle among non-target shapes and identified whehter the letter inside the target was a T or L with a button-press. A distractor was defined as a non-target shape containing a target-related letter (T or L), whereas a neutral stimulus containing a non-target letter (F or P). On half of the trials, the distractor appeared as a color singleton, and on the other half, it shared the same color as the other stimuli, allowing congruency effects to be measured. If the color singleton was suppressed before its letter identity was processed, the letter inside the singleton distractor should not interfere with target identification, resulting in the elimination of the congruency effect. Behaviorally, response times were faster on singleton-present trials. Moreover, the congruency effect was eliminated when the distractor appeared as a singleton but remained significant when it did not, indicating effective suppression of singleton distractors. Supporting this interpretation, lateralized ERP analyses revealed an early distractor positivity (Pd; 100–150 ms) that was specific to singleton distractors, indicating that the singleton distractor was actively suppressed before its letter identities were processed. Consistent with this interpretation, EEG decoding showed stronger target-location representations on singleton-present trials, indicating that singleton distractors produced less interference with target processing. Together, the behavioral, ERP, and EEG decoding results demonstrate that singleton distractors were rapidly and efficiently suppressed, thereby reducing distractor interference and enhancing target processing.

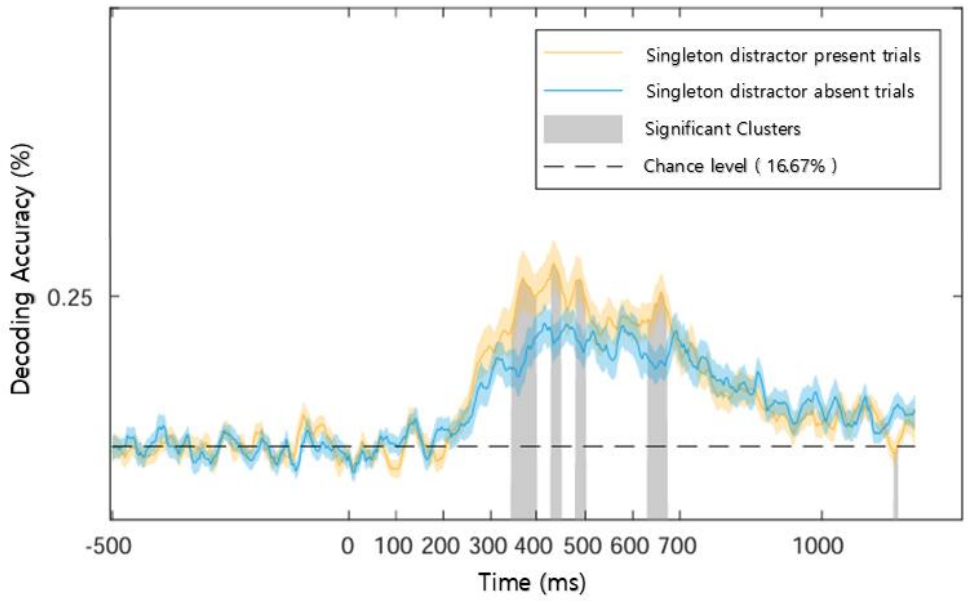

Figure 1. ERP-based decoding of target location in singleton-distractor present and absent trials. Decoding accuracy for target location based on ERP activity is shown separately for singleton-distractor present trials (yellow line) and singleton-distractor absent trials (blue line). The dashed line indicates chance-level performance (16.67%), and the gray shaded regions indicate time windows showing significant differences between conditions

[#26]

Neural and Behavioral Effects of In-Phase Frontoparietal Theta tACS on Working Memory in Middle-Aged Adults

Hyeong Ha Kim[1], HeungSik Yoon[1], Jungmin Oh[1], Seoyeong Bhin[1], Sang Hee Kim[1]

[1]Department of Brain and Cognitive Engineering, Korea University, Seoul, Korea

Working memory declines with age, and transcranial alternating current stimulation (tACS) has been proposed as a promising approach to enhance working memory. In particular, in-phase theta tACS applied to frontal and parietal regions is thought to enhance phase synchronization between these regions, thereby facilitating interregional communication underlying working memory processes. As working memory decline becomes noticeable in middle-aged adults, the present study investigated whether five sessions of in-phase theta tACS could improve working memory performance in adults aged 50–65 years and modulate neural activity and representations associated with memory processing. Participants were 40 healthy adults aged 50-65 years assigned to active (n=19) or sham (n=21) groups. At pre- and post-intervention, participants completed a verbal n-back task and a word pair recognition task during fMRI, as well as a visual n-back task and the Self-Ordered Pointing Task (SOPT) outside the scanner. The intervention consisted of five sessions of adaptive n-back training combined with in-phase theta tACS applied to the left dorsolateral prefrontal cortex (DLPFC; F3) and the left inferior parietal lobule (IPL; P3) for 20 minutes per session. The active group showed greater improvement in adaptive n-back performance from session 1 to session 5 than the sham group, although this difference did not reach statistical significance. No significant group differences were observed in the other behavioral tasks. In the neural data, compared with the sham group, the active group showed reduced activation in the right anterior cingulate cortex (ACC) for the 2-back > 0-back contrast and increased neural representational similarity between the stimulated regions (left DLPFC and left IPL) from pre- to post-intervention. Although behavioral improvements were limited, these findings suggest that multi-session in-phase theta tACS may modulate neural processing and facilitate more efficient neural recruitment during working memory performance in middle-aged adults.

[#27]

Post-Conflict Adjustments Following Infrequent Responses: A Drift Diffusion Modeling Approach

Jaewon Han[1], Yang Seok Cho[1]

[1]School of Psychology, Korea University, Seoul, Korea

Biased response frequency induces response conflict by creating competition between a prepotent tendency to execute the frequent response and the response required on the current trial. Behaviorally, this conflict produces two sequential adjustments: overall response slowing after an infrequent-response trial, referred to as post-conflict slowing, and a reduced effect of current-trial response frequency following an infrequent relative to a frequent response, referred to as the frequency sequence effect (FSE). We hypothesized that these effects reflect two complementary post-conflict adjustments in the decision process: an increase in response threshold and a reduction in the preexisting bias toward the frequent response. Forty participants performed two alternating frequency-biased two-choice reaction time tasks, in each of which one stimulus–response pair occurred more frequently (75%) than the other (25%). To test our hypothesis, four drift diffusion models were fitted separately to each participant's response time and accuracy data. Across the models, boundary separation (Model 1), starting point (Model 2), both boundary separation and starting point (Model 3), or boundary separation, starting point, and nondecision time (Model 4) were allowed to vary as a function of previous-trial response frequency. Models incorporating both boundary separation and starting point adjustments successfully accounted for both post-conflict slowing and the FSE. Parameter estimates from Models 3 and 4 showed that boundary separation was significantly greater following an infrequent than a frequent response ($p < .001$), whereas the starting point shifted significantly away from the frequent-response boundary ($p = .020$). These findings suggest that frequency-based response conflict recruits at least two complementary control adjustments: a global increase in response caution and a selective reduction in bias toward the prepotent frequent response.

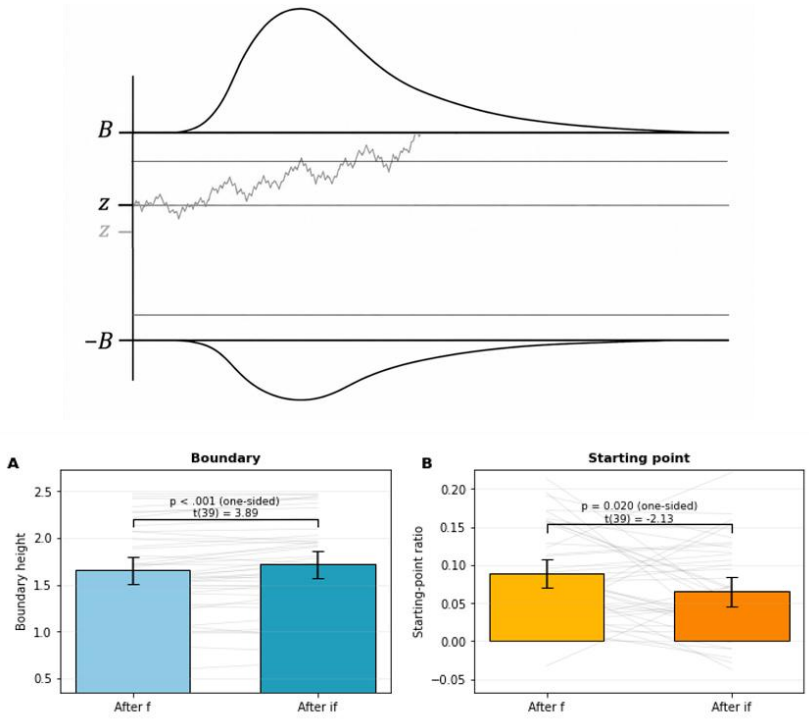

Figure 1. Changes in Boundary Separation and Starting Point Following Infrequent Responses in Model 3.

[#28]

Functional brain asymmetry reveals heterogeneous subtypes in autism spectrum disorder

Chaeyeon Kim[1,2], Sunghun Kim[1,2], Bo-yong Park[1,3]

[1]Department of Brain and Cognitive Engineering, Korea University, Seoul, Korea
[2]BK21 Four Institute of Precision Public Health, Seoul, Korea
[3]Center for Neuroscience Imaging Research, Institute of Basic Science, Suwon, Korea

Heterogeneity is as a critical factor in understanding inter-individual brain and behavioral variability in autism spectrum disorder (ASD). Since individuals with ASD exhibit atypical communication and social interaction skills closely linked to brain lateralization, this study investigated ASD heterogeneity using an asymmetry index that captures interhemispheric differences in brain function. Degree centrality was computed from the functional connectivity matrix and its asymmetry was quantified for each brain region. Using an unsupervised clustering algorithm, we identified three distinct subtypes within the ASD population that showed significant differences in brain asymmetry in the somatomotor, frontoparietal, and default mode networks. Comparisons of symptom severity indicated that subtype 2, which displayed atypical asymmetry patterns along the sensory-default mode axis, exhibited higher clinical severity. Functional connectivity analyses further revealed that subtype 1, characterized by rightward asymmetry, demonstrated hypoconnectivity across sensory and heteromodal association regions, whereas subtype 3, characterized by leftward asymmetry, exhibited hyperconnectivity. Cognitive decoding suggested distinct neurocognitive profiles for each subtype: subtype 1 was associated with increased engagement of self-referential and motivational processes (social-motivational subtype), subtype 2 with impaired regulatory and executive functions (cognitive control/impulsive subtype), and subtype 3 with enhanced involvement of mnemonic and language-related systems (memory-language subtype). Together, these findings advance our understanding of functional brain heterogeneity in ASD and demonstrate that subtype identification based on hemispheric asymmetry offers a promising framework for elucidating topological and behavioral variability within the ASD population.

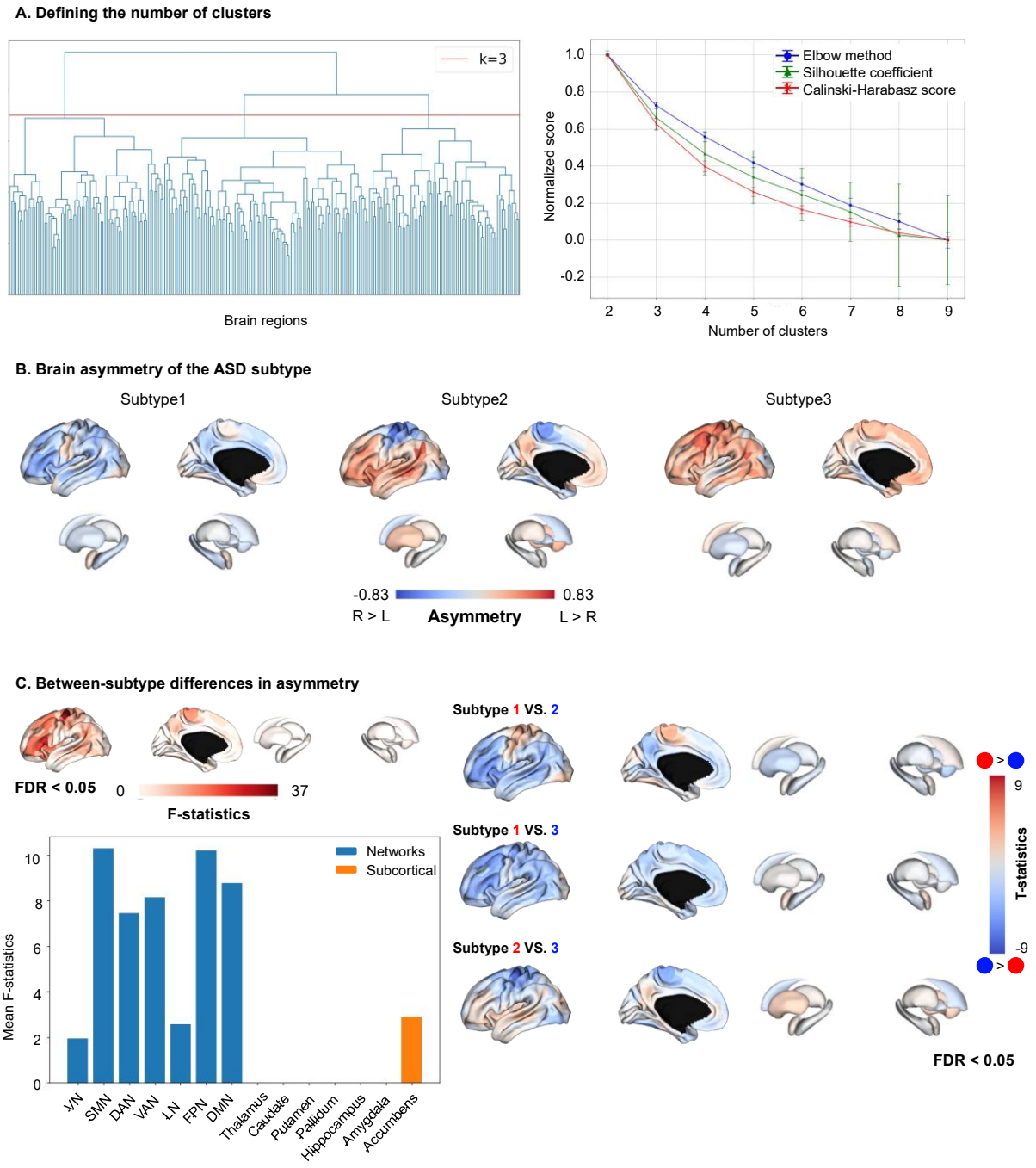

Fig. 1. Subtype identification within ASD. (A) Hierarchical clustering dendrogram showing three clusters delineated by the red line (left). Line plots display the Elbow method, Silhouette coefficient, and Calinski-Harabasz score for various cluster numbers (right). Error bars represent the mean and standard deviation across iterations. (B) Degree centrality asymmetry maps for each ASD subtype are visualized on brain surfaces. (C) F-statistic values showing regions with significant between-subtype differences in asymmetry are shown on brain surfaces, stratified by functional brain networks and subcortical regions (left). T-statistic maps from pairwise subtype comparisons are shown on the right. Abbreviations: ASD, autism spectrum disorder; L, left; R, right; VN, visual network; SMN, somatomotor network; DAN, dorsal attention network; VAN, ventral attention network; LN, limbic network; FPN, frontoparietal network; DMN, default mode network; FDR, false discovery rate.

[#29]

Cognitive Learner Profiles in Repeated L2 Grammar Practice: A Machine-Learning Approach Using SVT and MAZE Tasks

Jeahong Kim[1], Sungyeop Ha[1], Yeri Cho[1], Kichun Nam[1]

[1]Department of Psychology, Korea University, Seoul, Korea

Repeated practice is central to second-language (L2) grammar learning, yet learners may not improve through a single common pathway. Some learners may become faster and more accurate, whereas others may remain slow but accurate, show persistent grammatical misconceptions, or become vulnerable to familiarity-based errors after repeated exposure. The present study examined whether repeated computer-based grammar practice can reveal distinct cognitive learner profiles in L2 English grammar learning. Korean learners of English completed repeated sessions of two complementary tasks: a Sentence Verification Task (SVT), which measured explicit grammatical knowledge, and a MAZE task, which measured online phrase-construction performance. Accuracy, reaction time, signal detection indices, learning-curve parameters, speed–accuracy patterns, and item-level error trajectories were extracted as learner-level features. A machine-learning-based profiling approach was used to identify latent learner types without imposing a simple high-versus-low proficiency distinction. Unsupervised clustering was first applied to examine whether learners naturally formed distinct performance profiles. Supervised prediction models were then used to test whether early-session indicators predicted later performance or later learner-profile membership. Feature-importance analyses were conducted to interpret which behavioral and cognitive indicators contributed most strongly to learner classification and prediction.

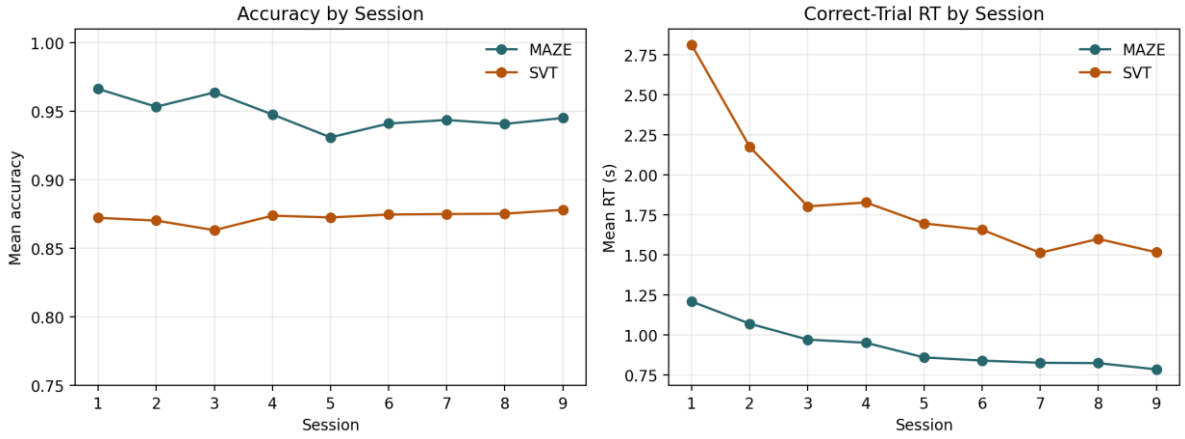

Figure 1. Accuracy, Correct-Trial RT by Session.

[#30]

REV-ERBα Activation Reduces Dopamine Release and Addictive Behavior

Jihyun Lee[1], June-Seek Choi[1], Yong Sang Jo[1,]

[1]School of Psychology, Korea University, Seoul, Korea

Drug addiction is associated with neuroadaptations in the brain's reward system, particularly dysregulated dopamine signaling. Because this dysfunction reflects altered regulation of the dopamine system, rather than moment-to-moment changes in neurotransmitter release, there is a need for molecular approaches that act upstream of synaptic transmission. Recent studies have shown that REV-ERBα transcriptionally represses tyrosine hydroxylase (TH), the rate-limiting enzyme in dopamine synthesis, thereby acting as a critical negative regulator of dopamine levels. Given this role, we hypothesized that targeting REV-ERBα could modulate dopamine dynamics and attenuate addictive behavior. Using fiber photometry with a genetically encoded dopamine sensor ($GRAB_{DA2m}$), dopamine (DA) activity in the nucleus accumbens (NAc) was measured during a sucrose lick test. We found that DA transients following reward delivery were significantly attenuated by a REV-ERBα agonist (STL1267), whereas a REV-ERBα antagonist (SR8278) significantly increased DA release. To determine whether bidirectional modulation of dopamine dynamics translates into changes in addictive behavior, cocaine self-administration (0.25 mg/kg/infusion) was established under fixed-ratio (FR) 1, FR3, and FR5 reinforcement schedules during daily 2-h sessions over 14 days. Thereafter, the REV-ERBα modulator was microinfused into the ventral tegmental area (VTA) 3 hours before sessions in which lever presses no longer resulted in cocaine delivery. Agonist treatment significantly accelerated the extinction of cocaine-seeking behavior, whereas antagonist treatment had no effect on extinction, with response levels remaining similar to control conditions. Taken together, our findings indicate that molecular modulation of dopamine synthesis via REV-ERBα effectively regulates reward-related dopamine signaling and suppresses addictive behavior, identifying REV-ERBα as a promising therapeutic target for addiction.

[#31]

Dissociable Neural Representations in mPFC Subregions during Self- vs. Other-Referenced Social Comparison

Sa Im Kim[1], Yuri Kim[1], Jinhee Kim[1], Wi Hun Jung[2]†, Hackjin Kim[1]†

[1] School of Psychology, Korea University, Seoul, 02841, Republic of Korea
[2] Department of Psychology, Gachon University, Seongnam 13120, Repulic of Korea

This study examined the neural mechanisms underlying social comparison by integrating goal orientation (self- vs. other-referential) and a regulatory focus (promotion vs. prevention) framework. Forty participants performed a cued response task across five conditions: be faster than self/other (promotion) or not slower than self/other (prevention), along with a control condition with no-feedback. While behavioral hit-rates showed no significant main or interaction effects, univariate fMRI revealed a robust self–other dissociation within the medial prefrontal cortex (mPFC). The rostral mPFC (rmPFC) was uniquely activated for the Self-Promotion vs. Self-Prevention contrast, whereas the dorsal mPFC (dmPFC) was uniquely recruited for the Other-Promotion vs. Other-Prevention contrast. Multivariate pattern analysis (IS-RSA) further elucidated how individual behavioral profiles modulate these neural patterns. K-means clustering of hit-rates identified two distinct phenotypes: self-focused and other-focused individuals. By correlating behavioral RDMs with neural RDMs for “Hit” conditions and applying the cluster-strength method, we identified cluster-specific parcels. Specifically, for both Self-Hit and Other-Hit contrasts, self-focused participants showed unique neural representations in vmPFC and pgACC/rmPFC, whereas other-focused participants showed unique representations in the dACC and dmPFC. These results suggest a clear anatomical and functional dissociation within the mPFC during social comparison. The rmPFC, linked to subjective value and self-relevant integration, specifically encodes self-related outcomes in self-focused individuals. In contrast, the dmPFC, associated with externally oriented evaluative processing, characterizes individuals focused on social-referential outcomes. Collectively, these findings provide evidence for a specialized mPFC architecture that navigates the complex interplay between individual regulatory goals and social comparison.

Figure 1A. fMRI Univariate Analysis

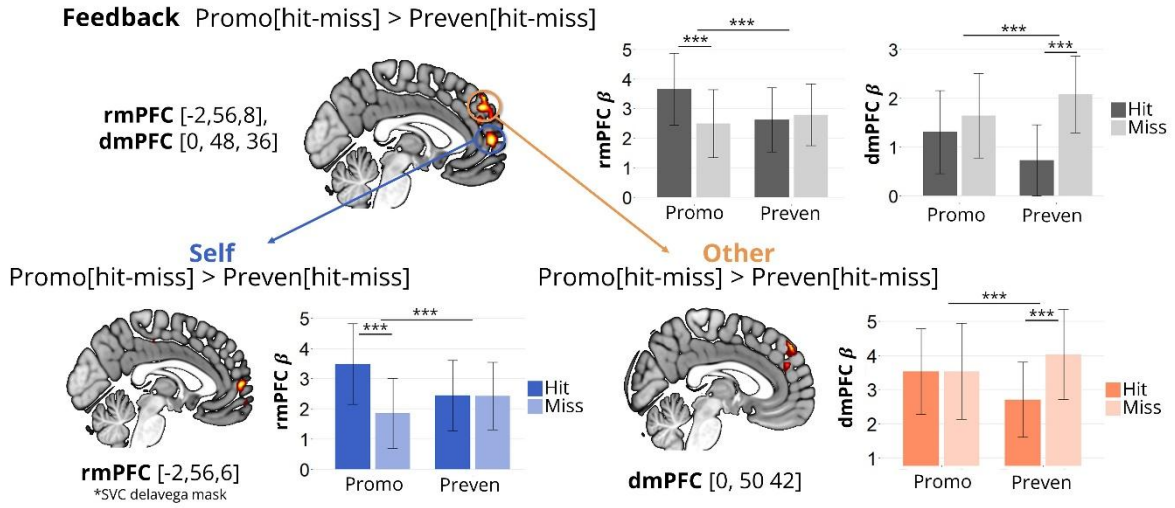

Figure 1B. fMRI Multivariate Analysis

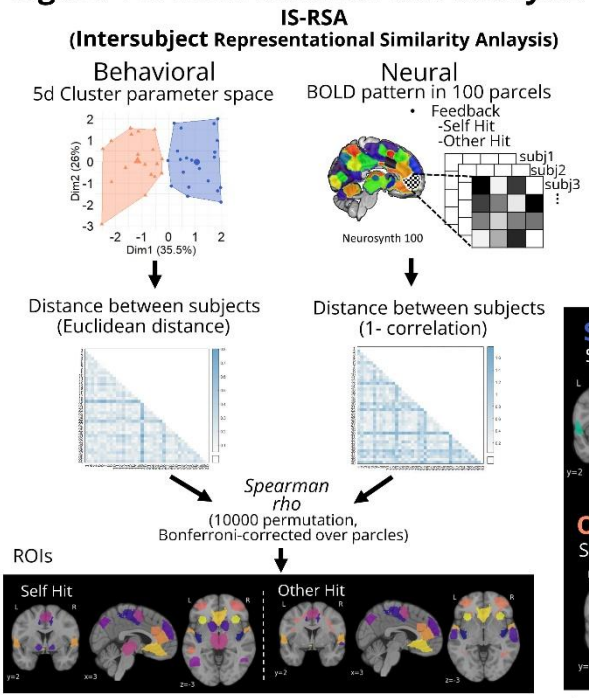

Regions where subjects with similar behavior strategy have similar 'Hit'-related BOLD pattern in Self,Other condition

Cluster strength score calculation

$$[-1, 1] \quad \text{cluster strength(cs)} = \frac{\overline{\text{between}} - \overline{\text{within}}}{\max(\overline{\text{between}}, \overline{\text{within}})}$$

cs > 0 :
between dissimilarity > within dissimilarity
→ within more similar

Each cluster's cs mean 5000 permutation
(sign permutation test, cs > 0) for each ROI

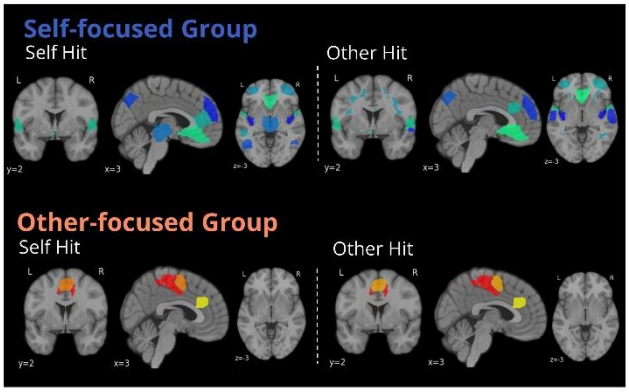

Cluster-specific regions where participants' activity patterns exhibited stronger similarity within their own cluster than across clusters.

[#32]

Modeling Reward Value- and Outcome Uncertainty-Driven Attentional Capture Using DDM

Jaein Lee[1], Yang Seok Cho[1]

[1]School of Psychology, Korea University, Seoul, Korea

This study investigated how reward value and outcome uncertainty jointly influence attentional capture and decision-making in a value-driven attentional capture (VDAC) task using the Drift-Diffusion Model (DDM). Although reward-associated stimuli are known to capture attention automatically, it remains unclear how expected reward value and uncertainty interact to determine attentional priority. To address this issue, participants completed a VDAC task in which reward value and uncertainty were manipulated independently. Behavioral performance was modeled using the DDM to identify the cognitive mechanisms through which these factors influence attentional selection.

Behavioral analyses provided relatively weak evidence for a conventional value-driven attentional capture effect but revealed a robust influence of reward uncertainty. Specifically, distractors associated with low uncertainty produced greater interference than those associated with high uncertainty, indicating that attentional priority depends not only on expected reward value but also on the predictability of reward outcomes. One possible interpretation is that processing highly uncertain reward associations requires greater cognitive resources, reducing the capacity of reward-related distractors to capture attention when both value and uncertainty must be represented simultaneously. To identify the underlying decision mechanisms, competing DDMs were compared using the Bayesian Information Criterion (BIC). The best-fitting model included reward value, uncertainty, and their interaction as predictors of drift rate, whereas models allowing these factors to modulate boundary separation provided substantially poorer fits. These findings indicate that reward value and uncertainty primarily affect the quality and efficiency of evidence accumulation rather than strategic adjustments in response caution. Parameter estimates revealed a significant main effect of uncertainty and a significant value-by-uncertainty interaction. Lower-uncertainty distractors reduced drift rates, indicating stronger attentional competition and less efficient evidence accumulation. However, this impairment was attenuated when the associated reward value was also low, demonstrating that the influence of uncertainty depends on the motivational significance of the distractor. Taken together, these findings suggest that value-driven attentional capture is not a fixed or purely automatic consequence of reward learning. Instead, attentional selection emerges from the interactive effects of reward value and uncertainty on the dynamics of evidence accumulation. By showing that these influences are expressed primarily through drift rate rather than decision threshold, the present study identifies early information-processing mechanisms as the primary locus through which selection history shapes attention and provides a computational account of how reward uncertainty modulates value-driven attentional capture. highlights the importance of early information-processing mechanisms in linking selection history and attention.

Table 1. Posterior Parameter Estimates from the Drift-Diffusion Model.

Parameter	M	SD	2.5%	97.5%	95% CI
v_0 (intercept)	3.857	0.132	3.615	4.143	[3.615, 4.143]
β_value	-0.048	0.094	-0.234	0.149	[-0.234, 0.149]
β_uncertainty	-0.157	0.082	-0.349	-0.008	[-0.349, -0.008]*
β_interaction	0.292	0.124	0.064	0.563	[0.064, 0.563]*
boundary (a)	2.256	0.357	1.704	2.940	[1.704, 2.940]
nondecision (t)	0.249	0.013	0.221	0.269	[0.221, 0.269]

Note. M = posterior mean; SD = posterior standard deviation; 95% CI = 95% credible interval (2.5th–97.5th percentile). Parameters whose 95% CI excludes zero are marked with an asterisk (*).

[#33]

Age-Related Differences in Working and Episodic Memory: Effects of Emotional Valence on Mean Performance and Within-Group Performance Heterogeneity

Jungmin Oh[1], Hyeong Ha Kim[1], Seoyoung Bhin[1], Heungsik Yoon[1,]

[1]Department of Brain and Cognitive Engineering, Korea University, Seoul, Korea

Age-related changes in memory function cannot be fully explained by average performance decline alone. Although episodic memory and working memory performance generally decrease with aging, the degree and timing of decline may vary across individuals. Meanwhile, the emotional valence of memory stimuli may influence attentional allocation, encoding, and retrieval processes. The direction and magnitude of this influence may differ depending on valence type, memory function, and age. The present study examined not only how emotional valence modulates average memory performance across age groups, but also how within-group performance heterogeneity varies across emotional conditions. Data from up to 243 Korean adults were analyzed. Participants completed a single-session online cognitive assessment including the Self-Ordered Pointing Task (SOPT) and N-back task for working memory, and the Word Recognition Task (WRT) for episodic memory. Emotional valence was manipulated in the SOPT and WRT using positive, negative, and neutral stimuli. Conventional scoring analyses revealed age-related performance differences across working memory and episodic memory tasks. Younger adults generally outperformed older adults in the N-back task, showing higher accuracy and d′, faster response times, and lower inverse efficiency scores. In the SOPT, younger adults also showed better working memory performance, including fewer total errors and higher memory span. In the WRT, younger adults showed better episodic memory performance than older adults, particularly in correct rejection of recombined pairs and associative recognition. Across tasks involving emotional stimuli, positive stimuli generally produced better performance than negative stimuli. Inter-subject representational similarity analysis further examined whether task-specific behavioral dissimilarity patterns differed across age groups, with permutation tests used to compare group-level performance structures. These findings suggest that memory aging is reflected not only in mean performance differences, but also in age-related changes in within-group performance heterogeneity, with emotional valence contributing differently across memory domains.

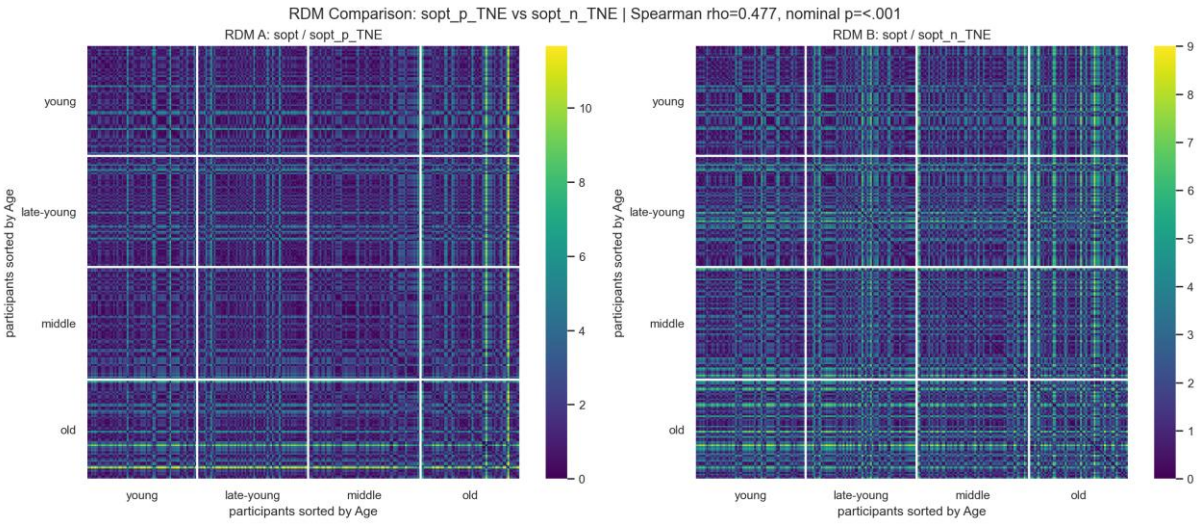

Figure 1. Inter-subject behavioral dissimilarity in SOPT total errors across emotional valence conditions. Participant-wise representational dissimilarity matrices (RDMs) were constructed separately for positive and negative SOPT total number of errors (TNE), with participants ordered by age group. Brighter colors indicate greater behavioral dissimilarity between participants. Within-group dissimilarity appeared to increase in older age groups, and negative stimuli showed greater heterogeneity than positive stimuli.

[#34]

Repetitive transcranial magnetic stimulation reorganizes functional connectome manifolds

Sunghun Kim[1,2], Se-Hong Kim[3], Bo-yong Park[1,4]

[1]Department of Brain and Cognitive Engineering, Korea University, Seoul, Republic of Korea
[2]BK21 Four Institute of Precision Public Health, Seoul, Republic of Korea
[3]Department of Family Medicine, St. Vincent's Hospital, College of Medicine, The Catholic University of Korea, Seoul, Republic of Korea
[4]Center for Neuroscience Imaging Research, Institute for Basic Science, Suwon, Republic of Korea

Repetitive transcranial magnetic stimulation (rTMS) is a noninvasive neuromodulation technique capable of modulating brain function. However, the large-scale network consequences of focal stimulation remain poorly understood. Here, we investigated whether high-frequency rTMS targeting the left dorsolateral prefrontal cortex (DLPFC) reshapes large-scale functional connectome organization. We analyzed resting-state functional magnetic resonance imaging data from a 4-week randomized, sham-controlled trial, in which participants received either active or sham rTMS. Functional connectivity gradients were estimated using manifold learning, and target-centered manifold differentiation was quantified as the Euclidean distance between each brain region and the stimulation site within manifold space. The rTMS group exhibited a spatially selective increase in manifold differentiation between the left DLPFC and the superior lateral temporal cortex, whereas no corresponding change was observed in the sham group. These findings indicate that rTMS increased the functional differentiation between the stimulation site and a distal association region. Cognitive decoding of intervention-related manifold changes further revealed associations with higher-order sensory and social-cognitive functions. Normative modeling demonstrated that this reorganization predominantly reflected a shift toward more typical patterns of brain connectivity, with stronger effects in the rTMS group than in the sham group. Together, these findings demonstrate that DLPFC-targeted rTMS reorganizes functional connectome architecture beyond the local stimulation site and suggest that manifold-based measures of connectome differentiation may serve as promising markers for future connectome-guided neuromodulation strategies.

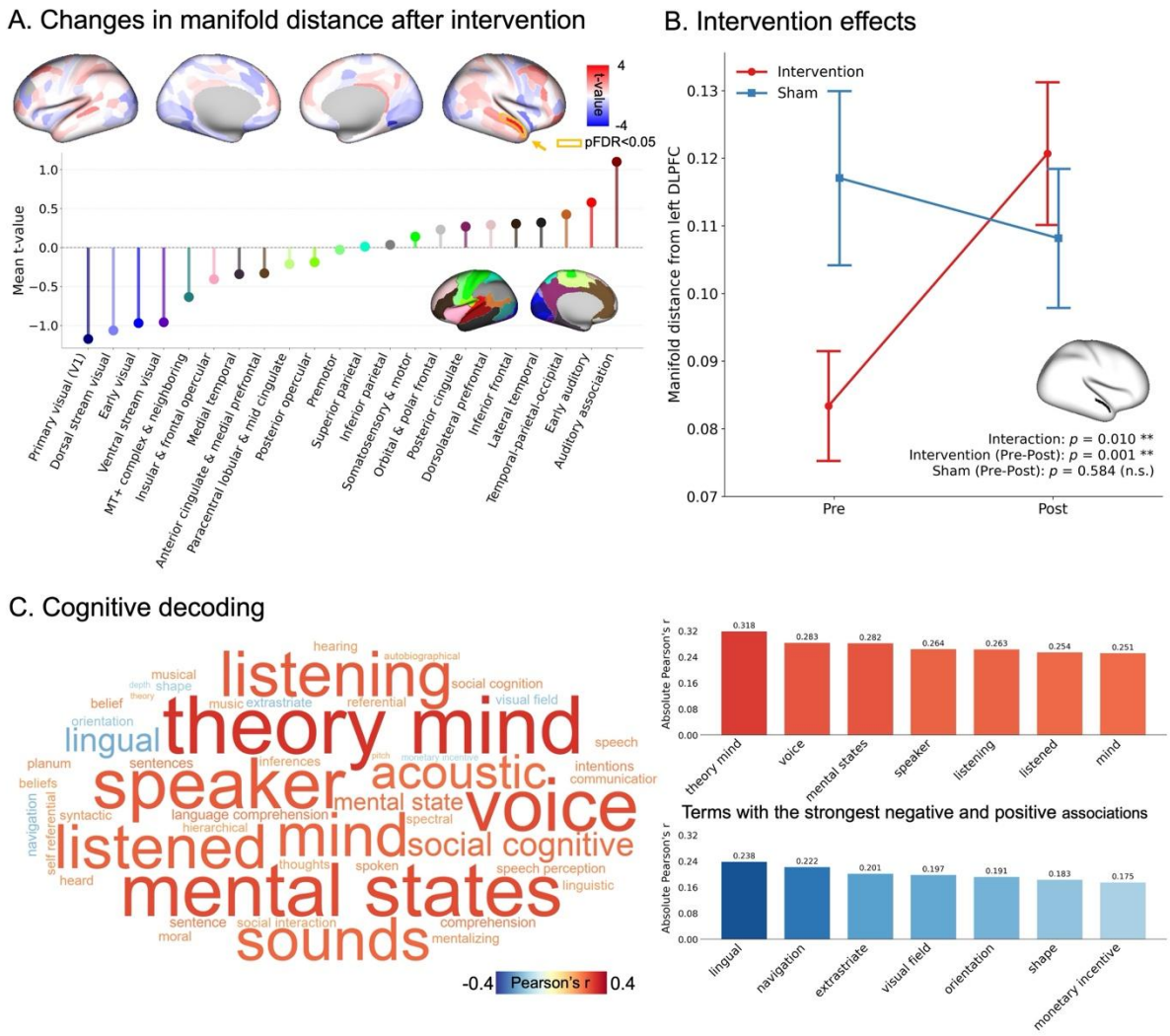

Figure. Intervention-related changes in manifold differentiation. (A) Changes in manifold distance from the left DLPFC following the rTMS intervention. Regions showing significant changes are outlined in yellow. Effects are stratified across 22 brain sections. (B) Group-by-time interaction effects in regions exhibiting significant changes in manifold distance after the intervention. (C) Cognitive decoding results associated with intervention-related changes in manifold distance. The top five positively and negatively associated cognitive terms are displayed as bar plots.

[#35]

The Impact of Time Pressure on Hierarchy-Based Conformity: The Moderating Role of Interoceptive Accuracy

Sanghun Kim[1], Daeeun Kim[2], Hackjin Kim[1]

[1]School of Psychology, Korea University, Seoul, Korea
[1]Department of Psychology, Korea Army Academy, Yeongcheon, Korea

Conformity is a process by which individuals adjust their judgments by incorporating others' opinions or preferences in social environments. Although individuals tend to conform more strongly to the opinions of superior than subordinate others, it remains unclear whether such conformity occurs in the same manner when decisions must be made within a limited amount of time. In addition, conformity may vary depending on how individuals process external social information and their internal states. The present study aimed to examine the effect of time pressure on hierarchy-based conformity and whether this effect is moderated by interoceptive accuracy (IAcc). Forty-four participants completed a hierarchy-based preference rating task. The results showed that participants exhibited lower overall conformity rates under high time pressure and conformed more to superior than subordinate partners. Importantly, the effects of time pressure and hierarchy information on conformity differed depending on IAcc. Participants with lower IAcc showed stronger conformity to superior partners under low time pressure, but this superior-directed conformity decreased under high time pressure. In contrast, participants with higher IAcc did not show a clear difference in conformity as a function of hierarchy. This moderating effect of IAcc was also confirmed in a trial-level logistic mixed-effects model that included IAcc as a continuous variable. Additional exploratory analyses showed that a self-report factor reflecting social-evaluative and empathic sensitivity also moderated conformity under time pressure. These findings suggest that conformity is not a simple and automatic response to others' preferences, but rather a social decision-making process involving time constraints, the partner's status, social evaluative concerns, and individual differences in internal bodily signal processing. The present study demonstrates that time pressure can constrain conformity in a hierarchical social context and that this effect may vary depending on individual differences in interoceptive accuracy.

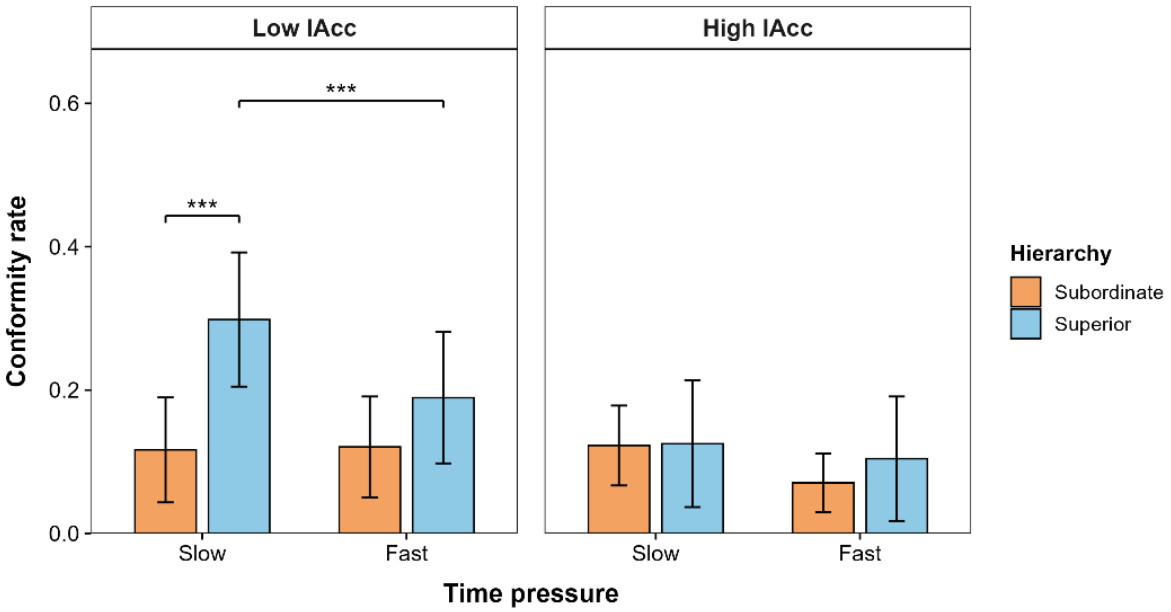

[#36]

Congruency Sequence Effects Optimize Real-Time Motor Correction in spatial Stroop Conflict

Yeong Sun Heo[1], Yang Seok Cho[1†]

[1]School of Psychology, Korea University, Seoul, Korea

How does cognitive control reshape an ongoing movement when stimulus location conflicts simultaneously with word meaning (S-S conflict) and response location (S-R conflict)? We recorded mouse trajectories from 31 participants who performed a spatial Stroop task in which they clicked the response box corresponding to the meaning of a directional word while ignoring its location. Continuous kinematic measures demonstrated robust automatic spatial capture before movement initiation on incongruent trials, with trajectories initially deviating toward the stimulus location before being corrected through compensatory acceleration. Prior conflict experience systematically reorganized the temporal dynamics of this capture-and-correction process. It did not alter movement initiation (4 ms, ns) but reduced movement time by 13 ms, indicating that sequential modulation operated through online motor correction rather than proactive response inhibition. Specifically, prior conflict reduced the magnitude of spatial capture by 17 px, advanced trajectory reversal toward the target by 20 ms and shifted peak velocity 19 ms earlier, reflecting more efficient compensatory acceleration. Time-resolved cluster analyses confirmed these effects across both early capture and late correction phases. Unlike the color Stroop task, where prior conflict primarily shortens initiation time through proactive task-conflict resolution, the addition of S-R conflict engages a qualitatively distinct control mechanism that optimizes the timing and efficiency of real-time motor correction.

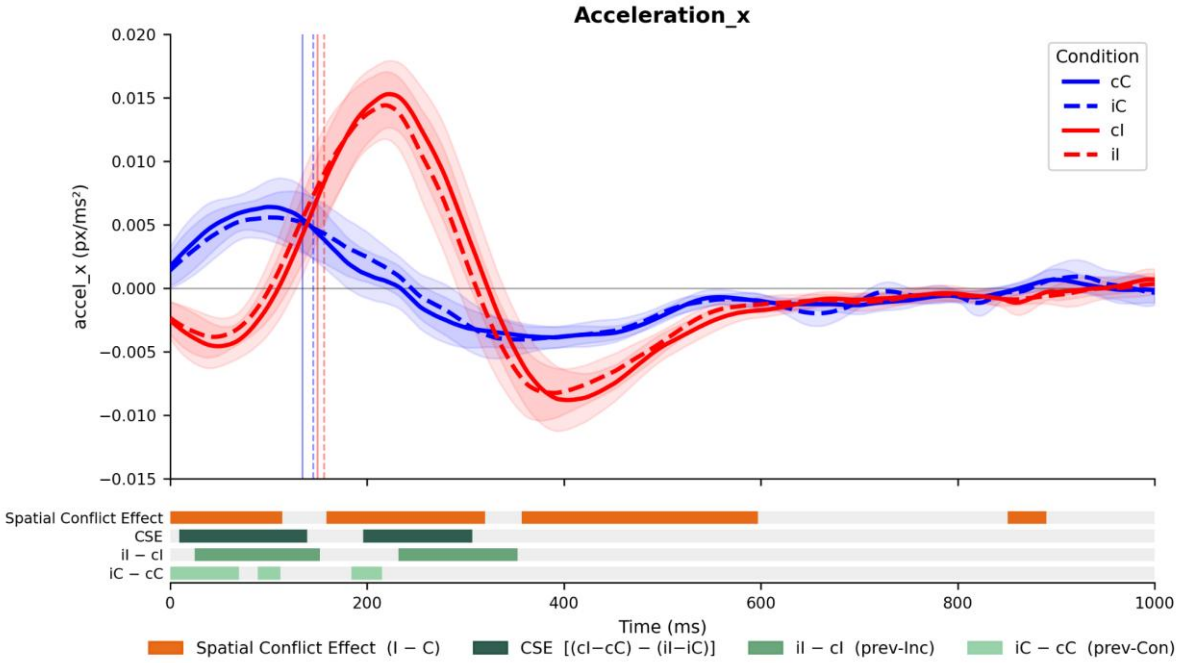

Figure 1. Time-Resolved Acceleration Profiles and Cluster-Significant Effects

[#37]

Validating the Mirroring Hypothesis: The Impact of Perceived AI Identity on Free-Form Conversational Engagement and Assimilation

Inseun Kim[1], Somin Park[1], Heuiseok Lim[2], June-Seek Choi[1]

[1]School of Psychology, Korea University, Seoul, Korea
[2]Department of Computer Science and Engineering, Korea University, Seoul, Korea

This study investigates how perceiving a conversational partner as an AI influences linguistic and emotional assimilation during unstructured interactions with Large Language Models (LLMs). By comparing user responses to an identically prompted ChatGPT-5 model labeled either as a 'Human Participant (C)' or an 'AI', we examined the effects of perceived identity on the communicative behaviors of both humans and AI chatbot. Results revealed that LLMs could extract information about their partners with high accuracy after unstructured conversations. However, despite being masked with a human label, the AI demonstrated a limited capacity to execute natural, fluid dialogue with humans. Interestingly, when participants explicitly perceived their partner's identity as an AI, they exhibited greater conversational engagement, actively contributing more to the dialogue and showing slightly higher levels of self-disclosure. These findings indicate that while LLMs still face constraints in seamlessly mimicking genuine human interaction, explicit awareness of an AI counterpart may paradoxically lower interaction barriers, prompting users to converse more freely and increase their communicative participation.

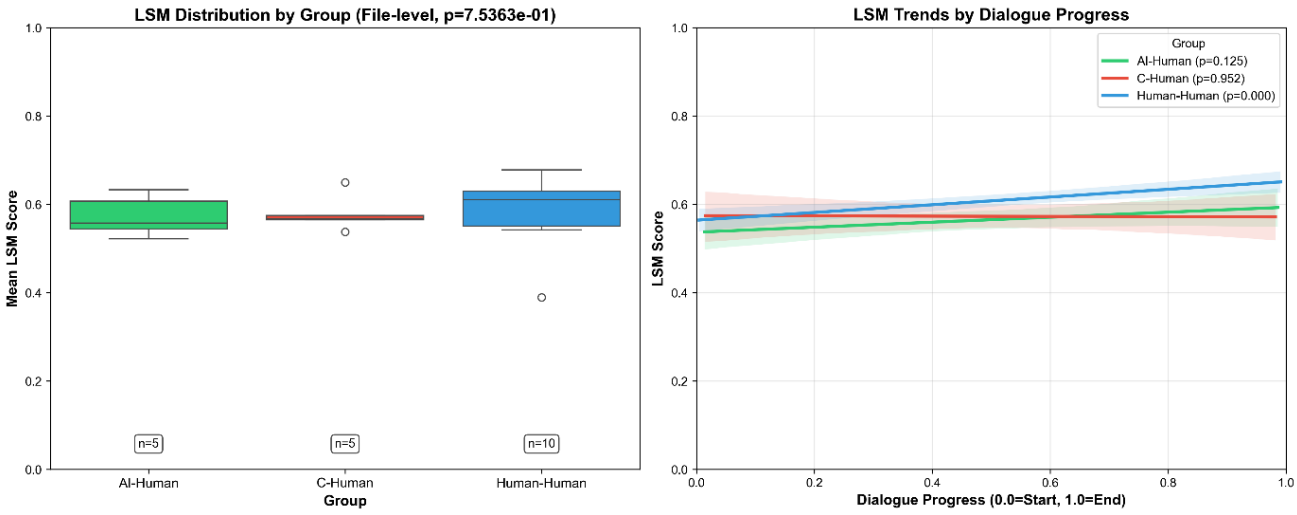

Figure 1. Comparison of LSM(Language Style Matching) distribution between groups.

[#38]

Ampakines CX516 and CX717 Selectively Enhance Cued Fear Learning, as Revealed by Behavioral Characterization

Seongmin Kwon[1], Yubin Seong[1], Kyeong Im Jo[1], June-Seek Choi[1]

[1]School of Psychology, Korea University, Seoul, Korea

Ampakines are positive allosteric modulators of AMPA receptors that have been proposed as potential cognitive enhancers due to their ability to facilitate excitatory synaptic transmission and promote long-term potentiation (LTP). Although previous studies have demonstrated beneficial effects of ampakines on cognition, it remains unclear whether these effects extend across distinct forms of associative learning and memory. To address this question, the present study examined the behavioral effects of two clinically relevant ampakines, CX516 and CX717, on cued fear conditioning, contextual fear conditioning, and spatial object recognition in healthy animals. In the cued fear conditioning paradigm, administration of CX516 (10 mg/kg) accelerated the acquisition of conditioned fear relative to vehicle treatment, although it did not alter asymptotic levels of conditioned freezing. In contrast, CX516 failed to enhance contextual fear conditioning under either immediate- or delayed-shock conditions and did not improve performance in the spatial object recognition task. To determine whether these findings generalized to a more potent ampakine, CX717 (1 mg/kg) was evaluated using the same behavioral paradigms. Consistent with the effects observed with CX516, CX717 facilitated cue-dependent fear learning while producing no measurable improvement in object recognition memory. Collectively, these findings suggest that ampakines preferentially enhance the acquisition of associative learning involving discrete sensory cues, whereas their effects on hippocampus-dependent contextual learning and declarative-like memory processes appear to be limited under normal physiological conditions.

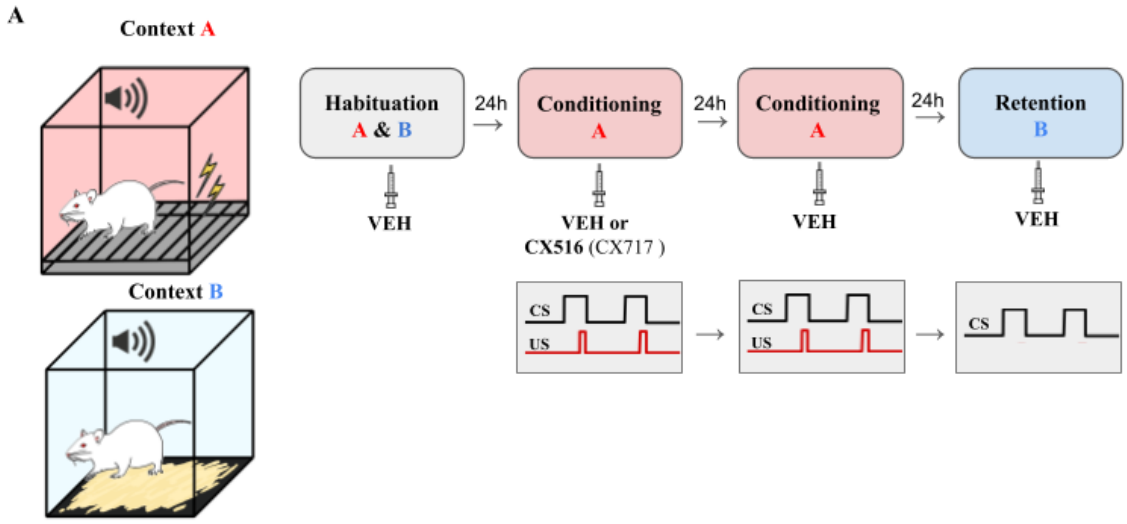

Fig. 1. Experimental design and behavioral procedure of cued fear conditioning with CX516 and CX717. (A) Schematic of context A and B used for cued fear condition, respectively (Cued FC). (B) Behavioral procedure of the Cued FC. (C) Schematic of Cued FC stimulation protocol: CS (2 kHz, 80 dB, 20 s) and US (1 mA, 0.5 s).

[#39]

Reliability-Aware Rejection over Multimodal Fusion for Camera and IMU-Based Respiratory Rate Estimation

Minwoo Lee[1], Chae Lynn Kim[1], Jungwoo Choi[1], Jong-Hwan Lee[1]

[1]Department of Brain and Cognitive Engineering, Korea University, Seoul, Korea

Respiratory rate (RR) is a clinically and behaviorally relevant marker of stress, cognitive load, and physiological deterioration. Both non-contact video-based methods, such as chest-motion optical flow, and wearable inertial measurement units (IMUs) have been used for respiratory monitoring. Although multimodal fusion is often reported to improve robustness, previous studies have mainly focused on contact-sensor fusion (PPG, ECG, IMU) or on combinations of non-contact sensors. The combination of frontal upper-body video and a body-worn chest IMU remains less studied, particularly for quality control based on cross-sensor information rather than a single sensor's internal quality. Five subjects completed 155 seated sessions across two tasks: slow regular breathing (BCT, ~5 bpm) and more irregular breathing under cognitive load (NCT, ~9.5 bpm). Each session recorded frontal upper-body video (30 fps), a chest-worn 6-axis IMU (~53 Hz), and an abdominal respiratory belt (10 Hz) as the reference. All signals were band-pass filtered (0.04-0.5 Hz) and analyzed using sliding FFT (60-s windows, 30-s steps), taking the dominant in-band spectral peak with harmonic correction to the fundamental frequency. Video RR was estimated from optical flow within a chest region of interest (MediaPipe, resPyre), whereas IMU RR was estimated from the first principal component of the normalized 6-axis signal. We evaluated direct fusion methods (confidence weighting, spectral product, learned gating) and reliability-aware rejection, in which video failure, defined as a discrepancy greater than 3 bpm from the belt, was predicted without the reference at test time from observable features including video SNR, spectral entropy, inter-method variance, video-IMU discrepancy, and temporal continuity. Unreliable windows were then rejected. The predictor was evaluated with leave-one-subject-out cross-validation (LOSO), and RR error was reported as subject-level mean absolute error (MAE) against the belt, by task. The video-based method achieved lower MAE than the IMU in both tasks: 0.37 versus 1.08 bpm in BCT and 1.56 versus 2.64 bpm in NCT. Direct fusion did not consistently improve over video alone; spectral fusion reached 1.51 bpm in NCT, comparable to the video-only result. An oracle selector choosing the better modality per window reached 0.64 bpm in NCT, indicating complementary information that was not reliably accessible through observable winner selection. Reliability-aware rejection was more effective: video failure was predictable without the reference (pooled LOSO ROC-AUC 0.915; training AUC 0.926), and rejecting unreliable windows reduced NCT MAE from 1.56 to 0.92 bpm at 84% coverage and overall MAE from 0.64 to 0.45 bpm at 96% coverage. Adding the IMU as a cross-check improved over video-only features, mainly through the video-IMU discrepancy feature (ablation ROC-AUC from 0.906 to 0.915). This benefit was stable across failure thresholds from 2 to 5 bpm. The video-based method was the strongest single modality, and direct point-estimate fusion did not outperform it. The chest IMU was nonetheless useful as an independent cross-check for reliability-aware rejection, suggesting that the second sensor's main value lies less in replacing or averaging the RR estimate and more in identifying unreliable video windows. Because rejection discards rather than recovers failed estimates, about 16% of NCT windows produced no accepted RR, with limited IMU fallback (MAE ~5.5 bpm). Future work should recover rejected windows and validate the approach in a larger cohort.

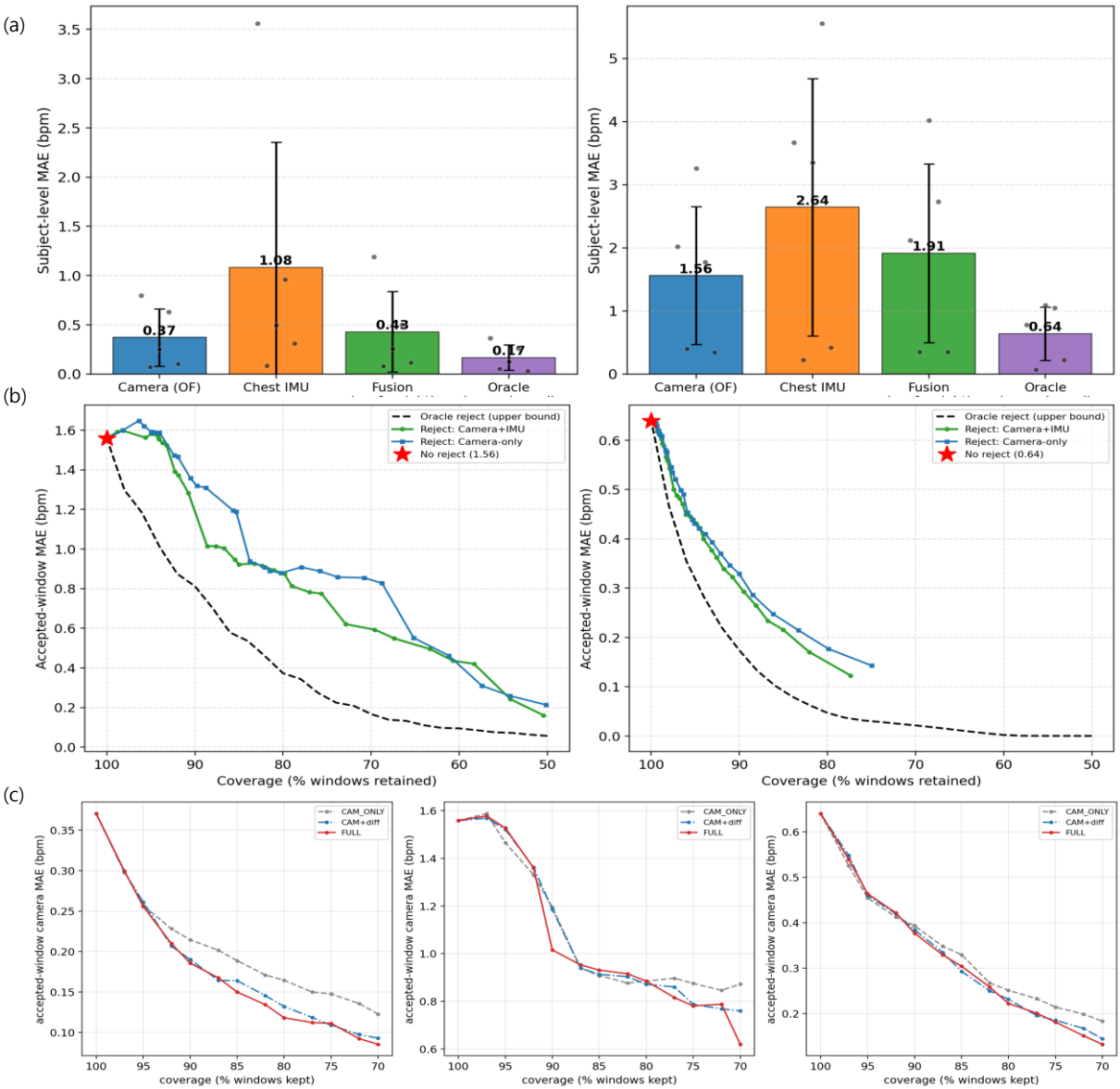

Figure 1. Seated respiration-rate estimation in five subjects, evaluated as subject-level MAE against the abdominal belt. (a) Per-task (BCT/NCT) MAE of camera optical flow, chest IMU, simple fusion by confidence weighting, and the oracle selector (performance upper bound). Bars indicate the across-subject mean, dots indicate individual subjects, and error bars indicate ±1 SD, clipped at 0. (b) Coverage–accuracy trade-off of reliability-aware rejection in NCT and all windows combined (ALL); lower coverage indicates stricter rejection. The dashed curve indicates the oracle-rejection bound, and the star marks no rejection. (c) Risk–coverage curves comparing failure-prediction feature sets: camera-only features (CAM_ONLY), camera features plus camera–IMU disagreement (CAM+diff), and the full feature set (FULL).

[#40]

Mobile-based facial emotion perception training (moFEPT) influences attentional processing

Sue Yeon Ko[1], Youn Joo Kwak[1], Yun jee Hwang[1], Jung Min Oh[1], Heung Sik Yoon[1], Sang Hee Kim[1*]

[1]Department of Brain and Cognitive Engineering, Korea University, Seoul, Republic of Korea

Individuals with higher aggressive tendencies often show hostile attribution bias, interpreting ambiguous social cues as hostile. This hostile attribution bias has been considered a key cognitive mechanism driving aggressive behavior. Facial expressions are critical cues for inferring others' emotions and intentions, and a tendency to interpret ambiguous expressions as anger may increase aggressive responses. Accordingly, interventions targeting facial emotion interpretation bias have been proposed. The current study examined whether facial emotion perception training can be effectively delivered in an online environment and whether such training influences attention bias toward emotional faces and behavioral measures of aggression. A total of 128 healthy adults aged 21-59 years completed a five-session online intervention over one week. Participants were randomly assigned to a training or a control group. The training intervention employed a feedback-based emotion perception task using morphed facial stimuli spanning a continuum from happiness to anger. In both groups, feedback was individualized based on each participant's pre-assessment responses. In the training group, feedback was adjusted to encourage happy responses to facial expressions containing slightly higher levels of anger relative to the individual balance point, whereas in the control group, feedback was matched to each participant's original balance point without inducing a perceptual shift. At pre- and post-intervention, participants completed an attention bias (AB) task and the point subtraction aggression paradigm (PSAP) to assess changes in attentional processing toward facial expressions of emotions and aggressive responding. Statistical analyses were conducted using difference scores (post minus pre) for each task. Results indicated that the online intervention effectively shifted facial emotion perception toward happiness in the training group compared to the control group ($F = 3.48$, $p = .035$). In attention bias, there was a group by emotion interaction. In orienting, attention goes more quickly to happy faces, in the training group ($p = .001$) and in disengagement, attention moved away faster from angry faces in the training group ($p < .001$). In contrast, no overall training-related reductions in aggressive behavior were observed on the PSAP. These suggest that (1) facial emotion perception training delivered online can bias emotion perception toward happiness over anger, (2) the training has the potential to alter attentional bias toward socioemotional cues. Further research is required to clarify the clinical significance and long-term effects of the training approach employed in this study.

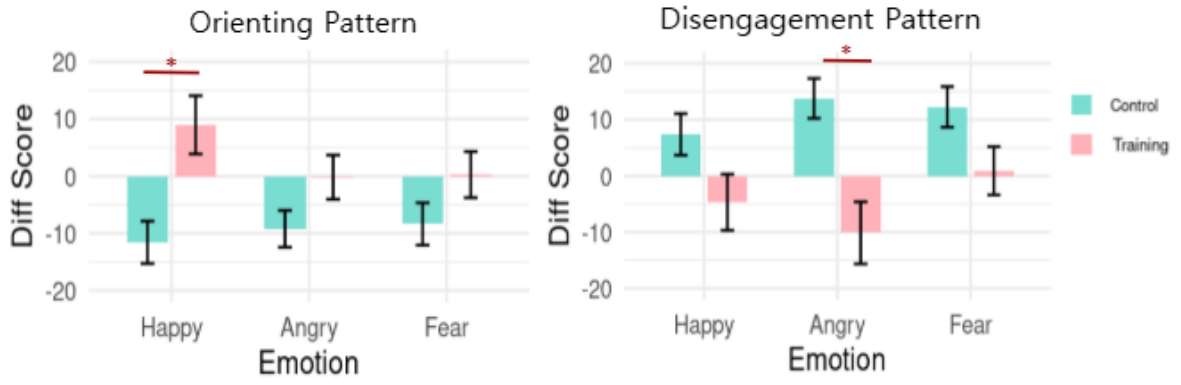

Figure 1. Group differences in attentional orienting and disengagement to emotional faces.

[#41]

Cortical responses to heartbeats predict alignment with group consensus in moral and affective preference

Juyoung Kim[1], Yuri Kim[1], Yoon Seo Lee[2], Yang Seok Cho[1], Hackjin Kim[1]

[1]Department of Psychology, Korea University, Seoul, Korea
[2]Department of Psychological & Brain Sciences, Washington University, St. Louis, USA

Moral judgments and affective preferences are influenced by social norms and group consensus, yet the mechanisms underlying this alignment remain poorly understood. Emerging accounts suggest that interoception—the processing of internal bodily signals—may contribute to the internalization of social norms by providing embodied signals that support value-based evaluations. However, the role of cortical responses to cardiac signals in preference alignment with group consensus has not been fully elucidated. The present study investigated how interoceptive accuracy (IAcc) and heartbeat-evoked potentials (HEP) contribute to individual differences in moral and affective preference alignment. Forty-one healthy individuals underwent EEG recordings during a resting state, a heartbeat counting task, a moral dilemma task, and a movie preference rating task. Preference alignment for each domain was quantified as the distance from group-level consensus for moral judgments and movie ratings. HEPs were time-locked to ECG R-peaks, and statistical significance was assessed using cluster-based permutation tests. Behaviorally, higher IAcc was associated with greater alignment with group consensus in moral judgments but conversely linked to more idiosyncratic choices in movie preferences. Neurally, frontocentral HEP amplitudes were enhanced during the heartbeat counting task and positively correlated with IAcc. Trial-wise analyses indicated that the association between HEP amplitude and preference distance varied as a function of IAcc. A frontocentral cluster showed positive correlations across tasks, while parietal clusters exhibited a positive correlation with moral distance but a negative correlation with movie distance. This study reveals the dual role of interoceptive processing: heightened sensitivity promotes moral conformity while fostering affective differentiation. Neurophysiologically, HEPs link cardiac–brain interactions to these domain-specific alignments. These findings provide a biological basis for how internal physiological signals modulate the balance between social integration and individual identity.

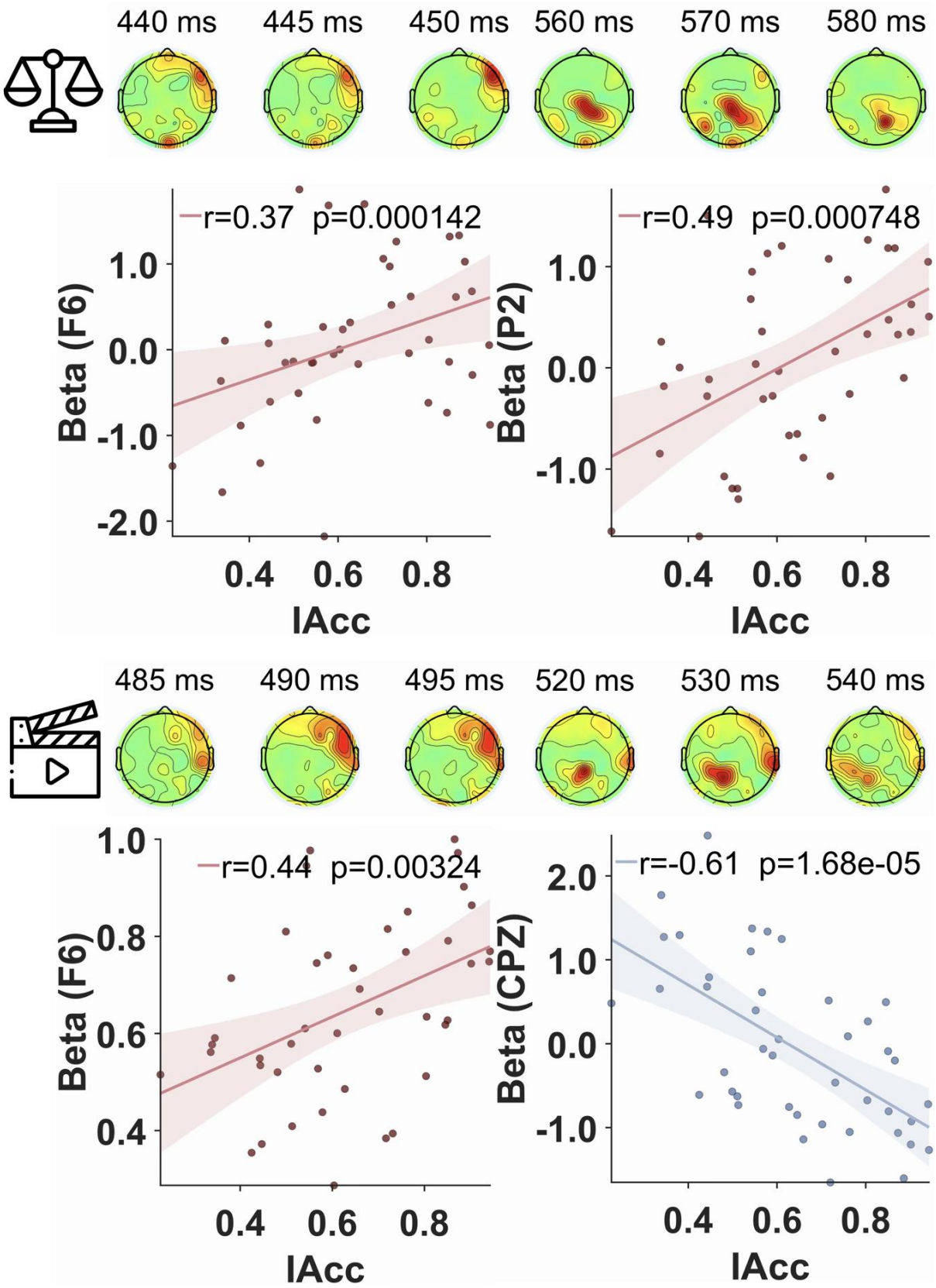

Figure 1. Task-related HEP for moral and affective decisions.

[#42]

Neural Mechanisms Linking Interoception and Subjective Preference: Evidence from EEG and fMRI

Yuri Kim[1], Jinhee Kim[1], Hackjin Kim[1]

[1]School of Psychology, Korea University, Seoul, Korea

Human preferences are shaped not only by external sensory input but by internal bodily states. Yet how the brain integrates cardiac signals into subjective value, and how individuals differ in regulating this process, remains unclear. Across two complementary experiments using electroencephalography (EEG) and functional magnetic resonance imaging (fMRI), we demonstrate that cortical responses to heartbeats—heartbeat-evoked potentials (HEPs)—linearly track subjective preference intensity, indexed by a frontal-positive to parietal-negative gradient. In parallel, fMRI revealed greater bilateral anterior insula (AIns) activation during preference decisions, which also encoded preference information even when it is task-irrelevant. Furthermore, metacognitive interoceptive awareness (metaIA) predicted both stronger HEP-preference coupling and reduced interference from task-irrelevant preference signals. Crucially, medial prefrontal cortex (mPFC)-insula connectivity mediated this behavioral linkage. Together, these findings establish that subjective preference is anchored in visceral afferent processing and that interoceptive metacognition enables flexible, context-dependent weighting of internal bodily signals during subjective value-based decision-making.

[#43]

Superlet-MAE: Self-Supervised Masked Autoencoding for Sleep Staging Using Single-Channel EEG

Jeong-Yun Cha[1,2], Choel-Hui Lee[1,2], Hakseung Kim[1] and Dong-Joo Kim[1]

[1]Department of Brain and Cognitive Engineering, Korea University, Seoul, Korea
[2]Interdisciplinary Program in Precision Public Health, Korea University, Seoul, Korea

Sleep stage classification is essential for diagnosing sleep disorders, but traditional polysomnography (PSG) is time consuming and labor-intensive and subject to inter-rater variabil ity, limiting its reliability. We propose a self-supervised learning (SSL) framework that integrates the Superlet Transform (SLT), offering high-resolution time-frequency analysis, with a Masked Autoencoder (MAE) architecture. Single-channel EEG signals (i.e., Fpz-Cz) from the Sleep-EDF dataset were transformed into Superlet scalograms and used for masked reconstruction pre training. Our method is the first to combine Superlet with MAE for EEG representation learning, enabling robust feature extrac tion from unlabeled data. Experimental results show that the proposed approach outperforms conventional transforms such as Short-Time Fourier Transform (STFT) and Continuous Wavelet Transform (CWT), achieving state-of-the-art performance in sleep staging. These findings highlight the potential of Superlet based SSL for scalable and accurate sleep analysis. The source code is available at https://github.com/chajy1212/Superlet-MAE.

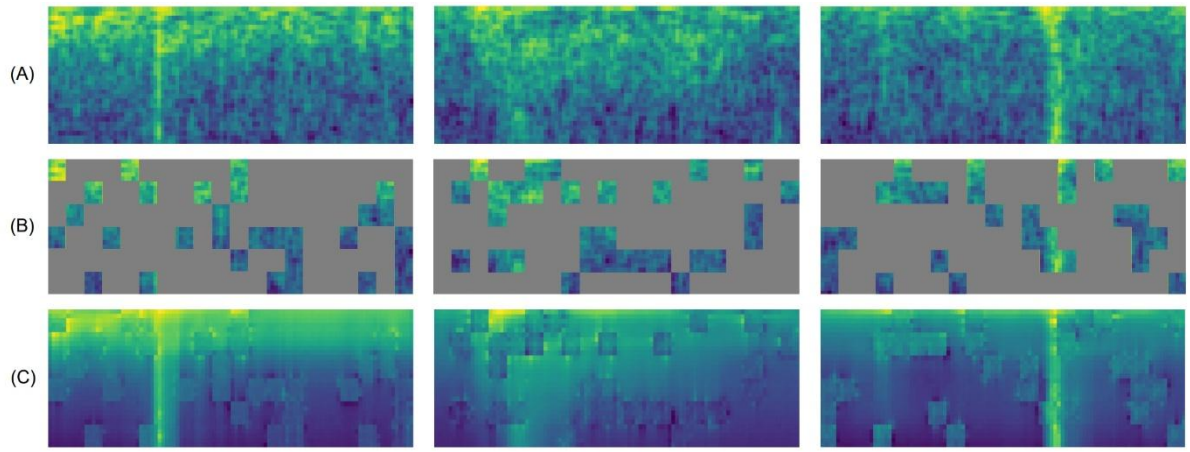

Figure 1. Visualization of MAE reconstruction performance (mask ratio = 0.75). (A) original scalogram, (B) masked scalogram, (C) reconstructed scalogram.

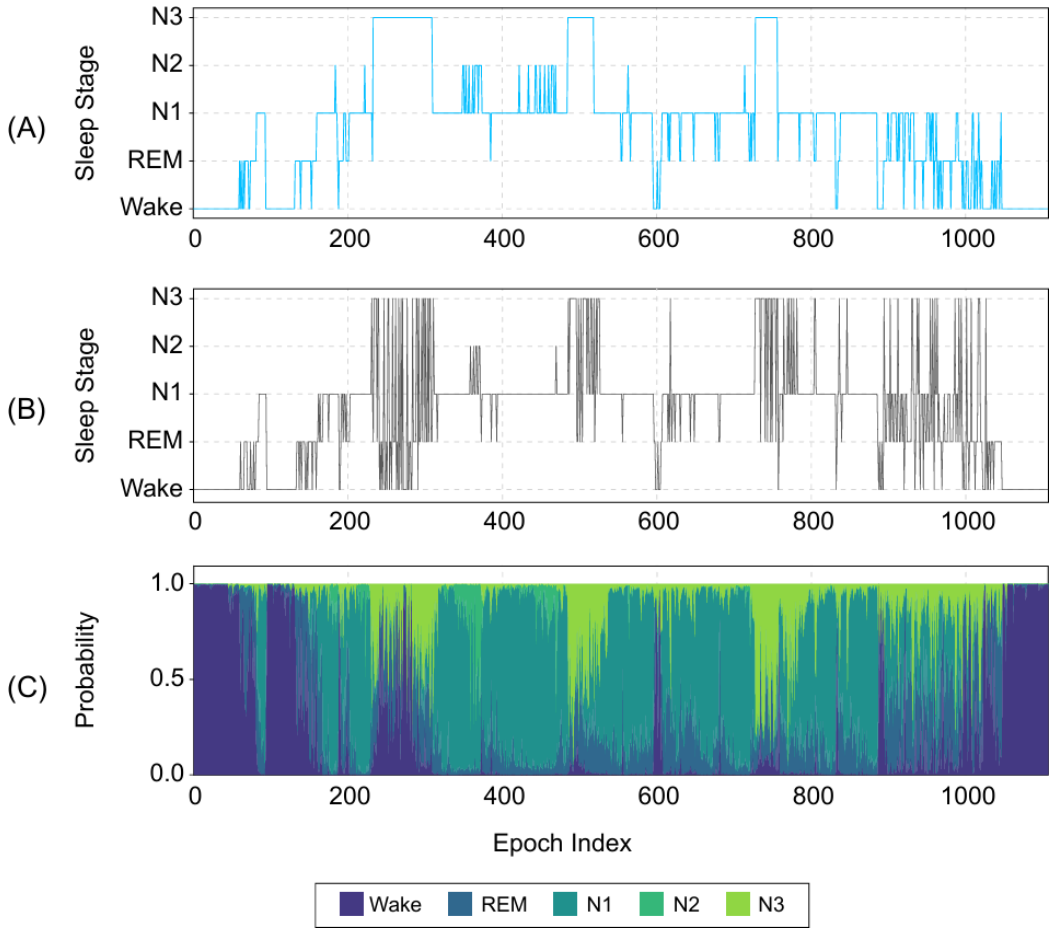

Figure 2. Visualization of sleep stage classification for subject #SC4632E0 in Sleep-EDFX. (A) ground-truth hypnogram based on manual annotations by sleep experts, (B) predicted hypnogram generated by the proposed MAE classifier, (C) softmax probability distribution across sleep stage over time.

Table 1. Model and training hyperparameters

Parameter	Value
Input Size	(30, 100)
Patch Size	(5, 5)
Input Channel	1
Masking Ratio	0.75
Epoch	300
Batch Size	512
Accumulation Step	1
Encoder Dim	256
Encoder Depth	20
Encoder Head	8
Decoder Dim	128
Decoder Depth	12
Decoder Head	8
Optimizer	AdamW
Learning Rate	1e-3

Table 2. Performance comparison of MAE using different time-frequency representations

Transform Type	Accuracy	Macro F1 Score	Cohen's Kappa
Superlet	**75.87% ± 1.39**	**63.23% ± 1.74**	**0.64 ± 0.02**
STFT	74.81% ± 1.27	61.74% ± 1.76	0.62 ± 0.02
CWT	75.45% ± 1.42	62.84% ± 1.16	0.63 ± 0.02

* STFT: Short-Time Fourier Transform analysis; CWT: Continuous Wavelet Transform

Table 3. Comparison with other SSL methods for linear evaluation using single-epoch EEG

Model	Accuracy	Macro F1 Score	Cohen's Kappa
Ours	**75.87% ± 1.39**	**63.23% ± 1.74**	**0.64 ± 0.02**
MAEEG [18]	72.29% ± 4.56	62.58% ± 6.02	0.62 ± 0.08
TS-TCC [27]	69.27% ± 8.15	54.09% ± 18.89	0.55 ± 0.15
BENDR [15]	70.73% ± 8.57	62.04% ± 8.03	0.60 ± 0.11

[#44]

Population analyses reveal heterogenous encoding in the medial prefrontal cortex during naturalistic foraging

Ji Hoon Jeong[1], June-Seek Choi[1]

[1]School of Psychology, Korea University

Foraging in the wild requires coordinated switching of critical functions, including goal-oriented navigation and context-appropriate action selection. Nevertheless, few studies have examined how different functions are represented in the brain during naturalistic foraging. To address this question, we recorded multiple single-unit activities from the medial prefrontal cortex (mPFC) of rats seeking a sucrose reward in the presence of an unpredictable attack posed by a robotic predator (Lobsterbot). Simultaneously recorded ensemble activities from neurons were analyzed in reference to various behavioral indices as the animal moved freely across the foraging area (F) between the nest (N) and the goal (E) area. An artificial neural network, trained with simultaneously recorded neural activity, estimated the rat's current distance from the Lobsterbot. The accuracy of distance estimation was the highest in the middle F-zone in which the dominant behavior was active navigation. The spatial encoding persisted in the N-zone when non-navigational behaviors such as grooming, rearing, and sniffing were excluded. In contrast, the accuracy decreased as the animal approached the E-zone, when the activity of the same neuronal ensembles was more correlated with events related to dynamic decision-making between food procurement and Lobsterbot evasion. A population-wide analysis confirmed highly heterogeneous encoding by the region. To further assess the decision-related activity in the E-zone, a naive Bayesian classifier was trained to predict the success and failure of avoidance behavior. The classifier predicted the avoidance outcome as much as 6 s before the head withdrawal. In addition, two sub-populations of recorded units with distinct temporal dynamics contributed differently to the prediction. These findings suggest that an overlapping population of mPFC neurons may switch between two heterogeneous modes, encoding relevant locations for goal-directed navigation or an imminent situational challenge.